Individual differences in honey bee behavior enabled by plasticity in brain gene regulatory networks

Beryl M. Jones[1,*], Vikyath D. Rao[2,3], Tim Gernat[2,4], Tobias Jagla[4], Amy Cash-Ahmed[2], Benjamin E. R. Rubin[5], Troy J. Comi[5], Shounak Bhogale[6], Syed S. Husain[7], Charles Blatti[2], Martin Middendorf[4], Saurabh Sinha[2,6], Sriram Chandrasekaran[7,8,‡], Gene E. Robinson[1,2,9,10,‡]

[1]Program in Ecology, Evolution, and Conservation Biology, University of Illinois at Urbana–Champaign, Urbana, IL, USA
[2]Carl R. Woese Institute for Genomic Biology, University of Illinois at Urbana–Champaign, Urbana, IL, USA
[3]Department of Physics, University of Illinois at Urbana–Champaign, Urbana, IL, USA
[4]Swarm Intelligence and Complex Systems Group, Department of Computer Science, Leipzig University, Leipzig, Germany
[5]Lewis-Sigler Institute for Integrative Genomics, Princeton University, Princeton, NJ, USA
[6]Center for Biophysics and Quantitative Biology, University of Illinois at Urbana–Champaign, Urbana, IL, USA
[7]Department of Biomedical Engineering, University of Michigan, Ann Arbor, MI, USA
[8]Center for Computational Medicine and Bioinformatics, University of Michigan, Ann Arbor, MI, USA
[9]Neuroscience Program, University of Illinois at Urbana–Champaign, Urbana, IL, USA
[10]Department of Entomology, University of Illinois at Urbana–Champaign, Urbana, IL, USA

*Present address: Department of Ecology and Evolutionary Biology, Lewis-Sigler Institute for Integrative Genomics, Princeton University, Princeton, NJ, USA
[‡] Joint corresponding authors, csriram@umich.edu and generobi@illinois.edu

Abstract

Understanding the regulatory architecture of phenotypic variation is a fundamental goal in biology, but connections between gene regulatory network (GRN) activity and individual differences in behavior are poorly understood. We characterized the molecular basis of behavioral plasticity in queenless honey bee (*Apis mellifera*) colonies, where individuals engage in both reproductive and non-reproductive behaviors. Using high-throughput behavioral tracking, we discovered these colonies contain a continuum of phenotypes, with some individuals specialized for either egg-laying or foraging and "generalists" that perform both. Brain gene expression and chromatin accessibility profiles were correlated with behavioral variation, with generalists intermediate in behavior and molecular profiles. Models of brain GRNs constructed for individuals revealed that transcription factor (TF) activity was highly predictive of behavior,

and behavior-associated regulatory regions had more TF motifs. These results provide new insights into the important role played by brain GRN plasticity in the regulation of behavior, with implications for social evolution.

Introduction

Understanding the genomic regulatory architecture of phenotypic plasticity is necessary to achieve comprehensive knowledge of the mechanisms and evolution of complex traits. While a growing body of knowledge exists on specific regulatory mechanisms involved in developmental plasticity, less is known about the regulation of behavioral plasticity. Behavioral plasticity is of special interest and presents unique challenges, as behavioral traits derive from the integrated actions of genetic, transcriptomic, and neuronal networks (Sinha et al., 2020).

Over the past 20 years, a close relationship between behavioral variation and brain gene expression has been documented across a range of organisms and behaviors (e.g., Zayed and Robinson, 2012). Still, the regulatory architecture underlying connections between the genome, brain, environment, and behavior are not well resolved, in part because behavior is itself a complex phenotype with substantial variation between individuals. To fully understand how genomic and transcriptomic variation is transduced into behavioral plasticity, we need both high-dimensional behavioral data at the individual level as well as information on regulatory genomics for those same individuals.

Modification of gene regulatory networks (GRNs) has emerged as an important driver of plasticity during the development and evolution of morphological phenotypes. For example, gains and losses of *cis*-regulatory elements (e.g., binding sites for transcription factors (TFs)) influence species-specific wing melanization patterns in *Heliconius* butterflies and *Drosophila* flies (Prud'homme et al., 2006; Reed et al., 2011; Werner et al., 2010). Pelvic loss in stickleback fish convergently evolved through deletion of a tissue-specific enhancer of the TF *Pitx1* in multiple natural populations (Chan et al., 2010). In other cases, similar morphological novelties arose independently through modification of distinct developmental programs, as observed for beak size variation across clades of finches (Mallarino et al., 2012). Recruitment of genes involved in developmental plasticity in the evolution of novel phenotypes is thought to be facilitated by the fact that TFs and other regulatory genes often have great temporal flexibility, with extensive variation in expression across developmental time (Dufour et al., 2020).

Similar to its role in morphological variation, plasticity in GRNs is theorized to influence behavioral variation, over both organismal and evolutionary time scales (Sinha et al., 2020). Brain gene expression is often responsive to environmental stimuli (Chandrasekaran et al., 2011; Cummings et al., 2008; Mukherjee et al., 2018; Rittschof et al., 2014; Whitfield et al., 2003) and the regulatory activity of many TFs is context-specific with respect to behavioral state (Chandrasekaran et al., 2011; Hamilton et al., 2019). In addition, modification of hormone signaling and GRNs in peripheral tissues has effects on brain GRNs and resulting behavior (Ament et al., 2012). These results demonstrate that GRNs are plastic not only across developmental timescales but also influence real-time behavioral variation. Still, the link between changes in GRNs and behavioral plasticity is weaker than for developmental plasticity (Sinha et al., 2020), and to our knowledge, no empirical studies have linked brain GRN plasticity to individual differences in behavior.

Eusocial insects are ideal for studying how GRN activity influences both developmental and behavioral plasticity at the individual scale. Eusociality is characterized by a reproductive division of labor between queen and worker castes, representing a developmentally plastic polyphenism well-studied in many species (e.g., Holldobler and Wilson, 1990; Michener, 1974; O'Donnell, 1998; Wheeler, 1986). Queens are specialized for reproductive functions, including mating and egg-laying, and in species with complex eusociality have levels of fecundity orders of magnitude greater than their solitary ancestors. Workers, on the other hand, typically do not perform reproductive behaviors and in many cases are sterile or unable to mate, instead performing many different non-reproductive behaviors in a colony that are essential for colony growth and development. Species with complex eusociality also often show additional within-caste behavioral plasticity, with individuals specializing on specific subsets of tasks based on differences in worker age, morphology, or genetic predisposition. The extensive behavioral plasticity observed in colonies of eusocial species may be linked to ancestral developmental plasticity (Kapheim et al., 2020), highlighting the interconnectedness of gene regulation in both developmental and behavioral phenotypes relevant for social behavior (Sinha et al., 2020).

We studied the relationship between brain GRN activity and behavior at the individual scale. We focused on a recently discovered, surprising form of behavioral plasticity among worker honey bees. Honey bee workers do not mate, but they possess functional ovaries and can produce viable haploid eggs. Laying workers (LW) are rare in queenright colonies (Ratnieks,

102 1993; Visscher, 1996) but frequent in situations of permanent queenlessness, when colonies lose
103 their queen and then fail to rear a replacement queen. In these cases, up to 50% of workers may
104 activate their ovaries (Sakagami, 1954) and some of these workers lay eggs, producing thousands
105 of drones prior to colony death (Page and Erickson, 1988). Recently, it was discovered that some
106 LWs engage in both reproductive and non-reproductive behaviors (Naeger et al., 2013), a level
107 of behavioral plasticity not previously described in honey bee workers. Studying honey bee
108 workers in LW colonies enables investigation of the molecular architecture of behavioral
109 variation typically only seen when comparing queens and workers, without the confounds of
110 caste-specific developmental and physiological differences.

111 Recent advances in machine learning and automatic behavioral tracking have enabled the
112 study of individual behavior for thousands of members within social insect colonies (Crall et al.,
113 2015; Gernat et al., 2018; Greenwald et al., 2015; Mersch et al., 2013; Wario et al., 2015; Gernat
114 et al. 2020). We used automatic behavioral tracking, genomics, and the extensive behavioral
115 plasticity present in honey bee colonies with LW to test the hypothesis that individual differences
116 in behavior are associated with changes in the activity of brain GRNs (i.e., changes in the
117 expression of TFs and their target genes). Our results provide key insights into the mechanisms
118 underlying the regulation of individual differences in behavior by brain GRNs.
119

120 **Results**

121 *Extensive variation in behavior across laying workers*

122 To define the behavior of individual bees, we deployed a high-resolution, automatic
123 behavior monitoring system on six LW colonies in which each bee (n=800 per colony) was
124 individually barcoded, similar to Gernat et al. (2018). Our extension of this system identifies the
125 location and heading direction of each individual once per second, and uses convolutional neural
126 networks and machine learning to detect behaviors (Gernat et al., 2020). For each individual
127 across seven days of tracking (when bees were 15-21 days old), egg-laying events and foraging
128 trips were detected from images of the hive interior and entrance (Figure 1A). A total of 115,281
129 egg-laying events and 96,086 foraging trips were predicted for the six colonies (Supplementary
130 File 1).

131 Colonies exhibited considerable variation in the proportion of bees engaged in egg-laying
132 and/or foraging. With the exception of colony F, more workers were identified as layers than

133 foragers (Figure 1B). Across all colonies, a high proportion of bees were observed laying eggs
134 (54% with at least two egg-laying events on at least one day) or foraging (28% with at least two
135 foraging trips on at least one day) during the recording period, while 10.8% of bees performed
136 both egg-laying and foraging on the same day at least once during the seven days of tracking. A
137 small number of these "generalist" bees (1.3%; 45 individuals) were exceptional in their
138 consistent high performance of both measured behaviors, with a minimum of two egg-laying
139 events and two foraging trips on the same day, across at least three days. Three-day ethograms of
140 an egg-layer, generalist, and forager are shown in Figure 1C. Ovary dissection of a subset of
141 individuals revealed that 100% of specialized egg-layers and generalists had active ovaries
142 (ovary scores of 3-5; Hess 1942), compared with only 54% of the specialized foragers (Figure
143 1D; Supplementary File 2). Of the foragers with activated ovaries, 13/14 had five or fewer
144 predicted egg-laying events, compared with generalists and layers, which laid an average of 206
145 eggs (range: 64-774).
146 The daily and lifetime behavior of each bee was summarized using two behavioral
147 scores: the "specialist" score, which describes how specialized an individual was on either egg-
148 laying or foraging, and the "generalist" score, which describes how much an individual
149 performed both egg-laying and foraging. Scores were derived from daily normalized ranks
150 within colonies to allow comparison across days and colonies with differing overall activity
151 levels; bees that performed neither egg-laying nor foraging across the experiment have both
152 specialist and generalist scores of 0. Scores were mapped onto a two-dimensional color space for
153 visualization of behavior over time (Figure 2A; Figure 2- figure supplements 1-2; Supplementary
154 File 1).
155
156 *Influence of worker source colony on behavior*
157 To study the influence of source colony (including genetics and development) on
158 behavior, experimental colonies were assembled with workers from different source colonies
159 headed by unrelated queens. A subset of source colonies (4/6) was pre-screened for worker egg-
160 laying in queenless laboratory cages and showed variation in the timing and extent of egg-laying
161 (Figure 2- figure supplement 3). Bees in colonies A-C were derived from colonies with naturally
162 mated queens. Queens of *Apis mellifera* mate multiply with up to ~20 males and produce
163 workers with a mix of paternal genotypes (Adams et al., 1977; Estoup et al., 1994; Lobo and

Kerr, 1993); workers derived from these colonies were therefore assumed to be a mix of many patrilines. In contrast, experimental colonies D-F were assembled of workers obtained from two different source colonies, each of which was headed by a queen artificially inseminated with the semen of a single different drone (SDI). Workers within each SDI source colony are highly genetically related compared with workers from a naturally mated queen colony (average relatedness = 0.75 due to haplodiploidy).

Using SDI colonies allowed us to more easily explore whether the genetic and environmental differences between source colonies would lead to segregation of reproductive and non-reproductive behavior when mixed into the same (queenless) environment. In both colonies D and E, which were replicates of the same two SDI queens' offspring, the behavior of workers differed considerably by source: one source colony (SDI 1) comprised the majority of foragers, while the other (SDI 2) contained the majority of egg-layers (Figure 1B; Figure 2-figure supplement 2). In colony F the two SDI source colony progeny contributed more equally to foraging, while the most specialized egg-laying bees were predominantly from just one source colony (Figure 1B; Figure 2- figure supplement 2, SDIs 3 and 4). However, even in colonies where SDI source was clearly influential, specialized foragers and layers were identified from both sources, indicating that colony genetics and development are not the only contributors to individual variation in the likelihood of performing these behaviors. Similar patterns of specialization were observed in colonies A-C and D-F (Figure 1B; Figure 2- figure supplement 2), indicating that they were not an artifact of decreased intracolonial genetic diversity.

Specialized behavioral groups are highly transcriptionally and epigenetically distinct

A subset of highly specialized foragers, egg-layers, and generalist individuals were selected from two experimental colonies (from only one source SDI each, to minimize genetic variation among individuals) for brain gene expression and chromatin accessibility profiling (Figure 2A). Sampled individuals were among those with the most extreme specialist and generalist scores within each colony, and were assigned to behavioral groups based upon their lifetime behavior. Principal component analysis (PCA) on behavioral data for these individuals shows these three groups are behaviorally distinct, with generalists intermediate and more variable than forager and layer groups (Figure 2B).

194 Consistent with strong behavioral differentiation, foragers and layers exhibited
195 widespread differences in brain gene expression, with differential expression of nearly half
196 (46%) of all genes expressed in the brain (Figure 2C; Supplementary File 3). Differences in brain
197 gene expression were much stronger between foragers and layers (4506 differentially expressed
198 genes, DEGs; FDR<0.05) than for generalists relative to the two specialist groups (648 generalist
199 vs. layer and 374 generalist vs. forager DEGs). Generalists shared transcriptional profiles of both
200 foragers and layers, with nearly all genes differentially expressed between generalists and either
201 specialized group also present on the forager vs. layer DEG list (Figure 2C).
202 Forager vs. layer DEGs were enriched for cytoplasmic translation and transport gene
203 ontology (GO) biological processes, along with many metabolic and biosynthetic processes
204 (Supplementary File 3; FDR<0.05). All enriched GO terms but one (114 of 115) were for genes
205 more highly expressed in foragers relative to layers (forager-biased genes). The only GO term
206 enriched in layer-biased genes relative to foragers, cytoplasmic translation, was also the only
207 enriched GO term for genes overexpressed in generalists relative to foragers. Similarly, GO
208 terms enriched in generalist-biased genes (relative to layers) included many of the transport
209 terms enriched among forager-biased genes (Supplementary File 3).
210 In addition to differences in brain gene expression, layers and foragers showed
211 differences in accessible chromatin in the brain based on the Assay for Transposase-Accessible
212 Chromatin using sequencing (ATAC-seq; Buenrostro et al., 2013). 1794 differentially accessible
213 peaks (DAPs; FDR<0.05) were identified between foragers and layers, proximal to 1207 genes
214 (Figure 2D; Supplementary File 4). Forager-biased DEGs and genes proximal to forager-biased
215 DAPs overlapped significantly, 1.2x more than expected by chance (p=0.01 for hypergeometric
216 test of overlap). Genes proximal to peaks of accessible chromatin (regardless of differential
217 status) were on average more highly expressed than genes without proximal peaks (p<0.0001,
218 Kolmogorov-Smirnov test), supporting a signal of transcriptional activation near ATAC-seq
219 peaks (Figure 2- figure supplement 4). No DAPs were identified for foragers relative to
220 generalists, and there were only 16 DAPs (assigned to 13 genes) for generalists relative to layers
221 (Figure 2D). These 13 genes also had DAPs for foragers relative to layers (Figure 2D). DAPs
222 between foragers and layers were enriched for 148 GO terms (FDR<0.05), including
223 developmental processes, morphogenesis, and metabolism (Supplementary File 4). Similar to
224 differentially expressed genes, GO enrichment signal came from those DAPs with a bias in

225 foragers (i.e., more accessible in foragers relative to layers); no significantly enriched GO terms
226 were identified from layer-biased peaks, despite 44% of differential peaks being more accessible
227 in layers compared to foragers.
228
229 *Brain gene expression and chromatin accessibility are correlated with behavioral variation*
230 Our high-resolution behavioral data allowed us to test whether molecular and behavioral
231 variation were connected not only at the group level, but for individuals as well. Using PCA, we
232 found that degree of individual behavioral specialization was significantly correlated with
233 measures of both brain gene expression and chromatin accessibility (Figure 2E-F). Among PCs
234 for gene expression, PCs 1 and 2, which explained 31.1 and 11.9% of the total variance in gene
235 expression, respectively, were significantly correlated with individual behavioral specialist score
236 (Figure 2E). Generalists showed intermediate values of these PCs, consistent with an
237 intermediate brain transcriptomic profile. Genes with extreme PC loading values (upper and
238 lower 5% of loadings) for PC1 were enriched for transmembrane and ion transport, functions
239 related to aerobic and cellular respiration, and energy transport (Supplementary File 5). PC2
240 extreme loading genes were enriched for processes relating to detection of light,
241 phototransduction, and sensory perception (Supplementary File 5). Extreme loadings for both
242 PC1 and PC2 overlapped significantly with DEGs in the pairwise comparison of layers and
243 foragers (PC1: RF=1.2, p=1.39e-06, PC2: RF=1.7, p=8.39e-91).
244 Similarly, PCA of chromatin accessibility data revealed PCs that were correlated with
245 behavioral variation. Accessibility PCs 2, 3, and 4 were all significantly correlated with the
246 individual behavioral specialist score (Figure 2F). Genes with extreme PC loading values for
247 each correlated PC showed enrichment for multiple GO terms, including biological processes
248 related to cell-cell adhesion, locomotion, axon guidance, neuron projection guidance, and
249 synapse organization (Supplementary File 6). Many GO terms (11 of 37) were enriched for
250 extreme loading genes of both PCs 2 and 3, while synapse organization was the only enriched
251 term for loadings of PC4.
252
253 *GRN activity links molecular and behavioral phenotypes*
254 To test the role of transcription factor (TF) and gene regulatory plasticity in the regulation
255 of LW behavioral phenotypes, we conducted TF motif analyses and brain GRN reconstruction

256 (Chandrasekaran et al., 2011), individualized for each bee. The activity of many TF modules
257 (TFs and their predicted targets) showed significant correlations with individual variation in
258 several behavioral metrics, including numbers of eggs laid (50 TF modules), number of foraging
259 trips (74 TF modules), and proportion of returning foraging trips with pollen loads (41 TF
260 modules) (Figure 3A; Supplementary File 8). At the individual level, 23 TF modules were
261 correlated with all 9 behavioral and physiological metrics (Figure 3- figure supplement 1;
262 Supplementary File 8). These behaviorally correlated TF modules include TFs involved in JH
263 signaling (usp, Kr-h1, and Blimp-1), histone acetylation (trx), neuronal remodeling (Kr-h1,
264 Hr51, trx), and circadian rhythms (opa and Hr51).

265 In addition to the correlations between TF module activity and behavior, many TF motifs
266 were enriched in peaks of differential accessibility or in the regulatory regions of DEGs between
267 specialized layers and foragers. 77 out of 223 motifs (functionally validated in *Drosophila*
268 *melanogaster*, Zhu et al., 2011) were enriched in layer vs. forager DAPs (q-val<0.01,
269 Supplementary File 7), and 14 motifs were specifically enriched in the regulatory regions of
270 forager-upregulated DEGs (q-val<0.2, Supplementary File 7). Nine motifs were common to both
271 sets (Figure 3B-C), including binding sites for TFs involved in regulating nervous system
272 development (hairy, side, sr, and klu), transcription (max/mnt), juvenile hormone (JH) signaling
273 (tai and tai/met), chromatin modification (trl), and circadian rhythms (cwo). These motifs were
274 centrally enriched within DAPs (Figure 3B), and showed two peaks of elevated binding
275 probability in the promoter regions of forager-biased DEGs, one ~3kb upstream of
276 transcriptional start sites (TSSs) and a second overlapping TSSs (Figure 3C). By contrast, only
277 two TF motifs were significantly enriched in the regulatory regions of specialist vs. generalist
278 DEGs (mad and ken, Supplementary File 7), and no motifs were enriched within DAPs between
279 generalists and either specialist group (Supplementary File 7), likely due in part to the small
280 number of DAPs distinguishing generalists and specialists (Figure 2D). Many of the motifs
281 enriched within DAPs or DEG promoters are binding sites for TFs that were themselves
282 differentially expressed, including cwo, tai/met, side, h, and sr (Supplementary File 3).

283 Across individuals, GRN activity was largely consistent within each behavioral group
284 (Figure 4A), with TF module activity most distinct between layers and foragers. The relationship
285 between TF expression and behavior was so strong that it was possible to predict individual
286 behavior based solely upon the expression of TFs in the brain using a machine-learning

287 algorithm and leave-one-out cross validation (Figure 4B; Figure 4- figure supplement 1). TF
288 expression correctly predicted 100% of foragers and 94% of layers. By contrast, it was not
289 possible to predict generalists based on brain TF expression (only 1 of 8 correctly classified).
290
291
292 *Comparative analyses of LW colony behavioral phenotypes and other social insect phenotypes*
293 The performance of both egg laying and foraging by individuals in LW colonies,
294 previously reported in Naeger et al. (2013), is unusual for honey bees; these behaviors are
295 otherwise confined to separate castes (queens and workers). This raises the question of whether
296 the mechanisms underlying LW behavior reflect caste-related molecular differences. We
297 compared our gene expression results to previous studies of queens, workers, and worker
298 subcastes in various species of social insects to ask whether the molecular architecture of LW
299 phenotypes may be useful in the context of understanding additional social phenotypes.
300 In comparison with honey bee subcastes, forager-biased genes in LW colonies showed
301 significant overlap with forager-biased genes in two studies of queenright colonies (when
302 compared with nurses) (RF=1.7 p=1.707e-09; Alaux et al., 2009; RF=1.9 p=1.740e-07; Whitfield
303 et al., 2003; Supplementary File 9). Layer-biased genes in this study overlapped with genes
304 upregulated in nurses relative to foragers in these queenright colonies (RF=1.7, p=3.656e-10;
305 Alaux et al., 2009; RF=2.0, p=1.116e-13; Whitfield et al., 2003; Supplementary File 9).
306 In addition, differences in brain gene expression between egg-layers and foragers
307 mirrored caste-related differences across species. Genes differentially expressed between
308 foragers and egg-layers in this study were enriched for previously identified queen vs. worker
309 brain DEGs in *Megalopta genalis* bees, which facultatively engage in both reproductive and non-
310 reproductive behaviors (RF:1.3, p=0.009; Jones et al., 2017; Supplementary File 9). Overlap was
311 in the expected direction, with queen-biased genes in *M. genalis* overlapping layer-biased genes
312 (RF:2.5, p=0.003) and worker-biased genes overlapping forager-biased genes (RF:1.6, p=0.01).
313 Further, worker-upregulated DEGs in the primitively eusocial wasp, *Polistes metricus*
314 overlapped significantly with forager-upregulated genes in this study (RF:2.6, p<0.0001; Toth et
315 al., 2010). In comparison with honey bee unmated queens and workers, overlap was significant
316 but in an unexpected direction: queen- and worker-biased genes overlapped with forager- and

317 layer- upregulated genes, respectively (RF:1.4, p=5.495e-08 and RF:1.2, p=0.008; Grozinger et
318 al., 2007; Supplementary File 9).
319 Additionally, forager vs. layer DEGs in this study were enriched for genes identified as
320 under selection in two studies of social evolution. Forager vs. layer DEGs overlapped
321 significantly with genes undergoing positive selection in honey bees (RF=1.1, p=0.015; Harpur
322 et al., 2014; Supplementary File 9) and across highly eusocial species relative to solitary or
323 primitively eusocial species (Woodard et al., 2011; Supplementary File 9). Genes under selection
324 in highly eusocial lineages were enriched specifically for genes identified here as upregulated in
325 foragers relative to layers (RF=1.4, p=0.009), but not for layer-biased DEGs (p=0.106)
326 (Supplementary File 9). Forager vs. layer DEGs were not significantly enriched for genes that
327 were identified in a third study as under selection in social lineages of bees (p=0.262; Kapheim
328 et al., 2015; Supplementary File 9). Many of the forager vs. layer DEGs also found to be
329 undergoing positive selection were related to metabolism (Supplemental File 9).
330
331 *TFs involved in LW plasticity previously implicated in social evolution*
332 Given that differences in brain gene expression between egg-layers and foragers reflect
333 caste-related differences, we also tested whether there is overlap between TFs involved in LW
334 plasticity and those previously implicated in social evolution. Indeed, many of the TFs we
335 identified above as related to behavioral plasticity based on motif enrichment, group predictive
336 analysis, or brain GRN activity were previously known to be associated with social behavior on
337 an evolutionary timescale. A comparative analysis of the genomes of ten bee species (Kapheim
338 et al., 2015) identified 13 TF motifs with associations between binding strength and social
339 complexity. Nine of those 13 motifs were also detected above as enriched within specialist DAPs
340 or DEG regulatory regions (p=0.015, hypergeometric test of overlap), and 6 of those 9 are
341 binding sites for TFs included in the above individualized GRNs. Along with TF module
342 correlation and behaviorally-predictive TF expression, these results highlight a set of 15 TFs as
343 compelling candidates in social plasticity and evolution, with significant associations in at least 3
344 of the 5 analyses (Figure 5; Table 1). The 15 TFs have functions related to known mechanisms
345 associated with social behavior, including brain development (Hamilton et al., 2016), JH
346 signaling (Woodard et al., 2011), and chromatin changes via histone acetylation (Simola et al.,
347 2015).

348

349 **Discussion**

350 Uncovering the regulatory mechanisms involved in behavioral plasticity is important to
351 fully understand how behavioral phenotypes develop and evolve. We used automatic behavioral
352 tracking and genomics to uncover the role of brain GRN activity in the extensive behavioral
353 variation observed in colonies of laying worker honey bees. We discovered that continuous
354 phenotypic variation is associated with continuous variation in both brain gene expression and
355 brain chromatin accessibility, and that TF activity is predictive of behavioral phenotype at the
356 individual level. These results provide new mechanistic insights into the important role played by
357 brain GRNs in the regulation of behavioral variation, with implications for understanding the
358 mechanisms and evolution of complex traits.

359 Our high-dimensional behavioral data revealed a near continuous distribution of
360 phenotypes along an axis of egg-laying and foraging, two behaviors that are typically expressed
361 separately in the queen and worker castes of honey bee colonies. Consistent with previous
362 reports of ovary activation in queenless colonies (Page and Erickson, 1988; Sakagami, 1954),
363 over half of workers tracked laid eggs. Some of these workers also engaged in foraging,
364 consistent with the observations of Naeger et al. (2013), which supports the suggestion that some
365 laying workers are not "selfish" reproducers but engage in activities that may benefit the colony
366 as a whole. We also showed a decoupling between ovary status and behavior for some
367 individuals, unlike what has been observed in many other social insect species (Barth et al.,
368 1975; Michener, 1974; Wilson, 1971). Two-thirds (14/21) of the foragers had activated ovaries,
369 but most laid eggs infrequently or not at all, demonstrating that ovary activation alone is not a
370 strong predictor of exactly which individuals will lay eggs. This decoupling of reproductive
371 physiology from reproductive behavior is consistent with the evolutionary co-option of
372 reproductive signaling pathways for non-reproductive behaviors, a phenomenon well
373 documented in honey bees (Tsuruda et al., 2008; Graham et al., 2011; Page et al., 2012). Given
374 previous demonstrations of cross-talk between peripheral tissues and brain gene networks in the
375 honey bee (Ament et al., 2012; Wheeler et al., 2013), our results further suggest that behavioral
376 variation in queenless workers likely involves the coordinated actions of multiple tissue types,
377 including the ovary.

Like the task specialization observed in typical, queenright colonies of honey bees and many other social insects (Oster and Wilson, 1979), the majority of individuals in LW colonies showed consistency in performance of either egg-laying or foraging, but not both. It is important to note that genetic variation may contribute to individual differences in behavior (Page and Robinson, 1991; Page and Robinson, 1994). However, the induction of egg-laying behavior in queenless colonies is itself a plastic response, suggesting that at least for egg-laying and generalist individuals, a combination of hereditary and environmental factors likely influence the development of these behavioral phenotypes. Task specialization can contribute to increased efficiency in social insects, either through learning or reduction of task switching costs (Holldobler and Wilson, 1990; Jeanson et al., 2008; Trumbo and Robinson, 1997; c.f. Dornhaus, 2008). In queenless colonies of honey bees, specialization along a reproductive/non-reproductive axis may lead to increased production of haploid males prior to the death of workers, with specialized foragers collecting food for these developing drones while specialized egg-layers work to produce thousands of drones synchronously in these terminal colonies (Page and Erickson, 1988). These findings suggest that LW honey bees may display a form of colony organization that is adaptive, as opposed to one of chaos and competition, which has long been thought to characterize LW colonies (Morse, 1990; Ratnieks et al., 2006; Ratnieks and Wenseleers, 2008; Dadant & Sons, 1975; Wenseleers and Ratnieks, 2006). Worker derived drones have viable sperm (Gençer and Kahya, 2011) and therefore may provide a permanently queenless honey bee colony with a final fitness opportunity if the males can successfully mate with queens. It is difficult to evaluate this hypothesis because the incidence of permanently queenless colonies is not known in natural populations of honey bees. However, production of drones by workers in LW colonies is similar to that observed in bumble bees, where worker competition over male production is a normal part of the colony cycle after queen death (Cnaani et al., 2002; Free, 1955), or even prior to queen death in some species (Velthuis and Duchateau, 2011).

Consistent with many other studies of behavior and brain gene expression across animal species (e.g., Bukhari et al., 2019; Mello et al., 1992; Whitfield et al., 2003), we identified robust brain transcriptional signatures associated with specific behavioral states. Beyond these group level differences, we also discovered that large components of this molecular variation were correlated with behavior, and both behavior and brain gene regulatory activity were continuous

409 across bees. Our finding that both brain gene expression and chromatin accessibility vary
410 continuously with behavioral phenotype suggests that behavioral plasticity is subserved by
411 continuously varying molecular programs, rather than threshold-based or quantized changes.
412 At the individual bee level, changes in the expression of TFs, accessibility of TF motifs
413 in enhancers and promoters, and activity of TF module target genes were all strongly associated
414 with behavioral state. This is highlighted by the results of our predictive analysis, where 97% of
415 specialists were accurately predicted to phenotype based on TF expression alone, despite the
416 small number of TFs relative to all differentially expressed genes. Spatial and temporal
417 integration of discrete events such as TF binding, aggregated at the whole brain level and across
418 TFs and genes, may lead to the continuous variation we observed in gene expression and
419 chromatin accessibility (e.g., Araya et al., 2014).
420 In addition to predicting the collective behavioral phenotypes of individual bees, our
421 analysis of GRNs allowed us to probe the influence of TF module activity on single behaviors.
422 We identified a set of 23 TF modules that were associated with all aspects of behavior and
423 physiology we measured. These TFs appear to coordinate sets of behaviors that are not overtly
424 linked (e.g., proportion of nectar foraging trips and number of eggs laid) but may be influenced
425 by the same regulatory machinery. Three of these modules are activated by TFs downstream of
426 JH, a hormone with numerous well-studied roles in social insect behavior, including the
427 regulation of oogenesis in queens and age-related division of labor in workers (Amdam et al.,
428 2008; Hamilton et al., 2017; Page et al., 2012). Our results are consistent with a role of JH
429 signaling in queenless colonies of worker honey bees, regulating a behavioral division of labor
430 between specialized egg-layers and foragers. These findings match previous work describing
431 differences in JH titers between egg-laying workers and foragers in queenless colonies
432 (Robinson et al., 1992), and suggest that mechanisms underlying variation in egg-laying
433 behavior may be similar to nurse/forager differences in queenright colonies. Overlap in brain
434 gene expression profiles between nurses and egg-layers further supports this conclusion.
435 By combining our analysis of GRNs in individual bees with motif enrichment in gene
436 regulatory regions across individuals, we identified a set of 15 TFs which appear to play a key
437 role in regulating specialist behavioral phenotypes (Figure 5). Intriguingly, many of these TFs
438 were also identified as relevant for social evolution, with increases in TF motif presence in gene
439 promoters of social compared with solitary species of bees (Kapheim et al., 2015). We observed

440 especially strong overlap of these evolutionarily-implicated TFs and those with motif enrichment
441 within differentially expressed genes or differentially accessible chromatin of specialist
442 phenotypes. This suggests that regulatory regions that arise during evolutionary transitions to
443 eusociality may be maintained and even further refined for the regulation of specialized
444 subcastes in social species. In contrast, comparatively little overlap was seen when comparing
445 evolutionarily-implicated TFs with TFs whose expression was most predictive of specialist
446 behavioral phenotypes. This mismatch between TF expression and motif presence may reflect
447 the complexity of GRNs, where genetic and epigenetic landscapes modulate the effects of TF
448 activity. Alternatively, these results may reflect differences in the mechanisms underlying intra-
449 vs. interspecific variation in social behavior. Further research exploring the role of these TFs and
450 their activity in a range of contexts is needed to provide clarity on these results.

451 While behavioral specialization appears to be common among members of queenless
452 honey bee colonies, the finding of even a small number of generalist bees who perform both egg-
453 laying and foraging has intriguing implications. The presence of these generalists suggests that
454 despite the long divergence from a solitary ancestor (~85 my, Branstetter et al., 2017), honey
455 bees retain great flexibility for performance of multiple behaviors that are typically confined to
456 either the queen or worker caste. Latent plasticity in social insects that is inducible under extreme
457 conditions is also seen in morphologically and temporally defined worker subcastes under
458 queenright conditions (Robinson, 1992; Simola et al., 2015; Wilson, 1980). Generalists showed
459 high variation in behavior, and similarly were difficult to predict phenotypically based on TF
460 activity, unlike specialists. Further, brain GRN activity in these individuals was less defined,
461 with fewer TF modules showing significant up- or down-regulation in generalist individuals
462 compared with specialists. Combined with PCA on brain gene expression and chromatin
463 accessibility, these findings suggest that generalists are molecularly intermediate between
464 specialized groups.

465 Our discovery of intermediate generalist phenotypes in laying worker colonies, along
466 with their molecular signatures, provides support for one of the leading theories of eusocial
467 evolution, the Ovarian Ground Plan Hypothesis (OGPH). The OGPH posits that the emergence
468 of queen and worker castes from solitary ancestors involved the genetic decoupling of
469 reproductive and non-reproductive behavioral programs through changes in gene regulation
470 acting on ancestral plasticity (Gadagkar, 1997; Turillazzi and West-Eberhard, 1996; West-

471 Eberhard, 1987). The phenotypic continuum we observed in laying worker colonies, with both
472 reproductive and non-reproductive specialists as well as generalists, suggests that this decoupling
473 process is at least partially reversible and/or incomplete in honey bees, unlike in eusocial species
474 where workers lack reproductive anatomy and corresponding behaviors entirely (e.g., ants and
475 higher termites). Additionally, molecular characterization of this behavioral variation, especially
476 our TF analyses, supports the hypothesis that incremental changes in gene regulatory network
477 activity led to the decoupling of solitary behavioral programs into distinct queen and worker
478 castes. This hypothesis is consistent with previous research linking changes in TF activity with
479 social evolution (Kapheim et al., 2015, 2020). If correct, this hypothesis provides a framework
480 for understanding the evolution of eusociality at the molecular level.
481

482 **Materials and Methods**

483 *Bees and colony setup*

484 Source colonies

485 Honey bee colonies were maintained according to standard beekeeping practices at the
486 University of Illinois Bee Research Facility in Urbana, Illinois. One-day-old adult worker bees
487 were obtained by removing sealed honeycomb frames of late-stage pupae from source colonies
488 in the field and housing them in an incubator inside emergence cages at 34 °C and 50% relative
489 humidity. Bees were removed from frames daily to collect adults less than 24 hours old.

490 Prior to establishing the colonies of barcoded bees, 16 source colonies were screened for
491 worker egg-laying ("laying worker", LW) potential by stocking Plexiglas cages with 50-100 one-
492 day-old workers and holding them in queenless, broodless conditions. Cages contained small
493 pieces of 3D-printed honeycomb (similar to Fine et al., 2018) to provide a standardized location
494 for workers to lay eggs, as well as 50% sucrose solution and pollen paste (45:45:10 ratio by
495 weight of pollen, honey, and water) provided *ad libitum* and refreshed daily. Cages were
496 monitored daily to count eggs. We found, as in other studies, variation in the timing and extent of
497 LW development among different source colonies (Fig. 2 – figure supplement 3), reflecting the
498 effect of genotypic and/or environmental differences on laying worker potential (Miller III and
499 Ratnieks, 2001; Page and Robinson, 1994; Robinson et al., 1990; Velthuis, 1970). When
500 possible, source colonies were chosen from among those screened that displayed high levels of
501 worker egg-laying in cages within 14 days.

502 To reduce genetic variation among bees used for sequencing, experimental colonies D-F
503 were established from a mix of two source colonies each headed by a queen of either *Apis*
504 *mellifera ligustica* or *Apis mellifera carnica* origin who had been artificially inseminated with
505 semen from a single drone (SDI) (queen rearing and inseminations performed by Sue Cobey,
506 Honey Bee Insemination Service; Washington State University; US stocks of bees are primarily,
507 but not completely *ligustica* or *carnica*). Experimental colonies A-C were established from
508 naturally mated, *Apis mellifera ligustica* source colonies. Honeycomb frames of late-stage pupae
509 were removed from source colonies and maintained in an indoor incubator. Worker bees were
510 collected from these frames each day to obtain 0-24 hr old individuals for barcoding. A total of
511 800 bees were used for each experimental colony, collected and barcoded over 1-2 days upon
512 eclosion (Supplementary File 10).

513 Barcoding bees

514 Bees were tagged with "bCode" barcodes as in Gernat et al. (2018). Unique sets of
515 bCodes were used to differentiate bees barcoded on different days, as well as to differentiate bees
516 from different source colonies in colonies D-F. To attach bCodes to bees, workers were
517 anesthetized on ice and then positioned using soft forceps (BioQuip, Compton, CA). A small
518 drop of Loctite Super Glue Gel Control (Henkel, Düsseldorf, Germany) was applied to the center
519 of the thorax of each bee, followed by a bCode positioned with its left and right edge parallel to
520 the anteroposterior axis of the bee. Bees were carefully placed in plastic dishes until they
521 recovered from cold anesthetization, at which point the glue was dry. After waking, all bees were
522 placed in a large container with Fluon®-coated walls (Insect-a-Slip, BioQuip) where honey was
523 provided *ad libitum* until placement into a custom observation hive, described below. At the end
524 of each barcoding day, bees were carefully transferred into the observation hive.

525

526 *Behavioral tracking*

527 Hive monitoring

528 Barcoded bees were housed in a glass-walled observation hive with a one-sided plastic
529 honeycomb frame, as in Gernat et al. (2018). Bees were unable to access the back side of the
530 honeycomb, and could exit the hive through a plastic tube to the outside. Colonies were
531 maintained in a dark room with a heater and humidifier that kept the room at approximately 32°C
532 and 50% relative humidity.

533 Infrared light (not visible to bees) was used to illuminate the hive from both the front and
534 back while capturing hive images. Images were acquired at one-second resolution with a
535 monochrome Prosilica GX6600 machine vision camera (Allied Vision, Stadtroda, Germany) fitted
536 with a Nikkor AF 135 mm f/2 D DC prime lens (Nikon, Minato City, Japan). Additional details
537 about image acquisition can be found in Gernat et al. (2018). Images were saved to a redundant
538 array of independent disks, then copied onto a computing cluster (Biocluster, UIUC) for analysis
539 after the end of each experimental recording period.

540 Entrance monitoring

541 Colonies of barcoded bees were given access to the outside via a tube connected through
542 an exterior wall of the Bee Research Facility to an entrance equipped with an automated flight
543 activity monitor as in Geffre et al. (2020). This monitor included a maze to slow down incoming
544 and outgoing bees, and a Raspberry Pi camera (5 megapixel v1.3, Adafruit, New York, NY) that
545 imaged the maze twice per second from 07:00 until 19:00 daily. The camera was controlled by a
546 Raspberry Pi 2B computer running the Raspian 8 operating system. Images were acquired using
547 the raspistill program and the following options: -n -ISO 400 -w 2593 -h 1400 -cfx 128:128 -x
548 none -e jpg -q 90 -tl 500 -t 595000 -bm.

549 *Barcode detection*

550 Barcodes were detected in hive images as in Gernat et al. (2018) and filtered to facilitate
551 subsequent behavioral analyses. Filtering involved removal of potential tracking errors, including
552 removal of barcodes that did not pass read error correction. In addition, records for barcodes that
553 were read twice in the same image were removed, as were hive image records of the same barcode
554 identified more than 5 cm/second between successive detections, which are likely to be
555 misidentifications. An average of 94.51% of detections remained after these filtering steps (range
556 across colonies: 91.94-97.11%). Finally, the time of death of each bee was estimated using the last
557 time she was observed for at least 4 minutes during a 5-minute window above the third row of
558 honeycomb cells from the bottom of the hive; dead bees tend to accumulate below this level prior
559 to being removed by other bees (Gernat et al., 2018). Records for bees following their time of
560 death were filtered out so behavioral scores (below) were calculated only over times in which bees
561 were alive.

562 In entrance monitor images, barcodes were similarly detected as in hive images, but with
563 parameters adjusted for images produced by the Raspberry Pi camera. Fast-moving bees were not

filtered out in entrance images, because bees do move quickly through the entrance monitor and due to the relatively small number of bees that fit into the maze, spurious fast movement due to bCode decoding errors is unlikely.

Egg-laying detector

Annotated image library

Hive images from three experimental colonies and across 12 different days were used for manual annotation of egg-laying events. The software Fiji (Schindelin et al., 2012) was used to mark the bCode positions of all workers laying eggs in an initial set of 1500 hive images, followed by an additional set of 782 images, each annotated by three independent observers. After the initial identification of egg-laying bees in these images, the two seconds before and after each egg-laying event were also annotated for those bees. Bees not marked as laying eggs with visible bCodes were considered non-egg-laying for training of the CNN, below.

CNN training and performance estimation

Two convolutional neural networks (CNNs) were trained on the annotated egg-laying images, using TensorFlow™ (Abadi et al., 2016). Methods are described fully in Gernat et al. (2020) and are presented briefly here. The first CNN used images cropped to include just a small rectangular region behind the barcode of each bee. For egg-laying bees, these images show the honeycomb, because their abdomen is backed into the comb and thus not visible. For non-layers, these images show the abdomen. The CNN was trained to differentiate between these two cases. The second CNN was applied to images of bees that were identified as potential egg-layers by the first CNN. It used slightly larger images that showed the entire bee and was trained to use information about the bee's posture and her immediate surroundings to identify false positives, which were subsequently filtered out.

Application of a CNN to an image results in a score between 0 and 1 that reflects the likelihood of that image showing the event of interest. Deciding whether a score is sufficiently high for assuming that the event took place involves thresholding that score. To choose thresholds for each CNN score and a minimum egg-laying duration, a calibration set of images, which were not used for training the CNNs, was used to estimate the performance of the egg-laying detector for different threshold combinations. Thresholds were chosen from this calibration set to maximize the detector's positive predictive value, then were applied to an independent test set of images that had also never been seen by the detector to obtain unbiased performance values. Based on the

performance estimation on the test set of images, the egg-laying detector had the following performance: 99.71% accuracy, 35.39% sensitivity, 100% specificity, 100% positive predictive value, and 99.71% negative predictive value. Minimizing false positives came at a cost to sensitivity, but bees who lay eggs will likely do so more than once over the course of the experiment and can thus still be identified as egg-layers (honey bees possess multiple ovarioles, each of which can develop eggs simultaneously (Hess, 1942)). Egg-laying detections were further aggregated into events: subsequent detections that occurred within 10 seconds and 11.2 mm (the width of two honeycomb cells) of one another were assumed to belong to the same egg-laying event and were merged.

Filtering and annotation of entrance data

Raw detections of bees in the entrance were filtered as in Geffre et al. (2020). Briefly, a bee must traverse at least one-third the distance of the entrance monitor to be counted, and traversals that occurred within 10 seconds of each other were merged into a single event. These traversal events were then determined to be incoming or outgoing based on the positional coordinates of the bee at the start and end times of each event. Numbers of foraging trips (Supplementary File 1) was inferred from series of outgoing and incoming events.

Incoming foraging trips were additionally annotated with trophallaxis data to determine whether a forager likely returned with nectar. CNNs trained to identify pairs of bees engaged in trophallaxis as well as the direction of trophallaxis (i.e., which bee was donor and which was recipient; Gernat et al., 2020) were used to annotate incoming trips for all bees. Parameters used for the detector resulted in the following performance metrics based on test images: 88.7% sensitivity, 99.6% specificity, 90.4% positive predictive value, 99.6% negative predictive value, and 88.9% accuracy in determining trophallactic role (donor or receiver) of each bee. If a bee was a trophallaxis donor within 5 minutes after returning from a trip (Seeley, 2009), with no trophallaxis reception prior to the donation, that foraging trip was annotated as a nectar trip. Additionally, incoming trips were manually annotated for pollen on the hindlegs of returning bees for colonies D-F. Combining these nectar and pollen data for each trip, the proportion of foraging trips with nectar ("p.nectar"), pollen ("p.pollen") or both ("p.both") were calculated per bee in these colonies.

Specialist and generalist scores

In order to characterize the activity of egg-laying and foraging for each bee, two behavioral scores were created. The "specialist" score describes how specialized an individual was on either egg-laying (scores near -1) or foraging (scores near +1) relative to other bees in the colony; bees that consistently performed both egg-laying and foraging, or that performed neither behavior, have specialist scores near 0. The generalist score ranges from 0 to 1 and describes the degree to which an individual performed both egg-laying and foraging behaviors, differentiating bees with specialist scores near 0 based on the performance (or not) of egg-laying and foraging. Scores were created by first counting the number of egg-laying and foraging events per day. Bees were then ranked for each behavior relative to other bees in the colony on the same day, with tying ranks being assigned the minimal rank (e.g., if three bees were tied between the 4th and 8th ranked bees, they all received a rank of 5). Ranks were then normalized by dividing by the maximum rank, so that all ranks were in the range [0,1]. The normalized rank space for each bee (i.e., normalized egg-laying rank and normalized foraging rank) was then mapped to behavioral scores (and corresponding color space) using the following formulae in polar coordinates (ρ,Θ) on the two-dimensional rank space: generalist score = $(1/2)\rho^2\sin^4 2\Theta$, specialist score= $\sin(\Theta-\pi/4)\rho^4\cos^4 2\Theta$. Note that the numerical value of the scores has no biological meaning, but is simply a mapping from rank space to the space of colors as shown in Figure 2- figure supplement 1.

Selection of bees for sequencing

The median of specialist and generalist scores was weighted to emphasize the latter part of the experiment; days 15-21 received a weight of 1-7, respectively, and each day's score was multiplied by this weight. These scores were used to characterize the overall behavior of each bee in the colony. The rank approach allowed for normalization across days with different overall levels of activity in the colony, and the median score across days provides an overall assessment of the lifetime behavior of each bee. These weighted median scores were used to rank all bees, and the top ranking specialists and generalists from two colonies were selected for brain RNA sequencing (RNAseq) and Assay for Transposase-Accessible Chromatin using sequencing (ATACseq). Scores for each sequenced bee (n=45, 25 from colony E, 20 from colony F), as well as total numbers of detected egg-laying and foraging events per bee, are provided in Supplementary File 2.

654 To examine variation in behavior within and among groups, principal component analysis
655 (PCA) was performed on the following set of behavioral traits (see also Supplementary File 2):
656 number of eggs laid, number of foraging events, proportion of trips with evidence of nectar
657 collection, proportion of trips with evidence of pollen collection, and proportion of trips with
658 evidence of both nectar and pollen. PCA was performed in R using the prcomp function and plotted
659 using the ggplot2 package.

660 *Tissue dissection and homogenization*

661 At the end of behavioral tracking, bees were collected from each colony and stored at -
662 80°C. All colonies were collected between 21:00-23:00 to ensure foragers were inside the hive.
663 For bees selected for sequencing, abdomens of each bee were carefully removed on dry ice and
664 incubated for 16 hours at -20°C in RNA-later ICE (Life Technologies, Carlsbad, CA). Ovaries
665 were imaged and assessed for ovary development using a 1-5 scale adapted from (Hess, 1942) to
666 assign an ovary score; a score of 3-5 indicates ovary activation. These dissections confirmed that
667 egg-layers and generalists had activated ovaries, while many foragers did not. Ovary scores, as
668 well as number of ovarioles as determined from dissections, are given in Supplementary File 2.

669 The head of each bee was freeze-dried at 300 milliTorr for 55 minutes, and whole brains
670 were removed from the head capsule in a dry ice ethanol bath (Schulz and Robinson, 1999).
671 Dissected brains were stored individually in 1.5 mL microcentrifuge tubes at -80°C until
672 extractions.

673 Brains were individually homogenized in 150 µL phosphate buffered saline (1X PBS,
674 Corning, Corning, NY, cat. #21-040-CV) with protein inhibitor complex (PIC, Complete Tablets,
675 EDTA-free Protease Inhibitor Cocktail from Roche, Basel, Switzerland, cat. #04693132001) using
676 a motorized pestle for 20 seconds. 50 µL of this homogenate was then pipetted into 450 µL cold
677 PBS+PIC and placed on ice for ATAC-seq library preparation (see below). The remaining 100 µL
678 homogenate was mixed with 500 µL RLT buffer (Qiagen, Hilden, Germany) with 1% β-
679 mercaptoethanol for use in the Qiagen RNeasy Mini Kit RNA extraction protocol (see below).

680 *RNAseq library preparation and sequencing*

681 Whole brain RNA was extracted from the 600 µL homogenate in RLT buffer after an
682 additional 30 second homogenization following the Qiagen RNeasy Mini Kit protocol, including
683 a DNase (Qiagen) treatment to remove genomic DNA. RNA quantities were determined for each

684 sample using a Qubit RNA HS Assay Kit (Invitrogen, Carlsbad, CA). High RNA integrity for all
685 samples was confirmed with Bioanalyzer 2100 RNA Pico chips (Agilent, Santa Clara, CA) prior
686 to library preparation.

687 RNAseq libraries were constructed and sequenced by the W.M. Keck Center for
688 Comparative and Functional Genomics at the Roy J. Carver Biotechnology Center (University of
689 Illinois at Urbana-Champaign). Libraries were constructed from 500 ng RNA per sample using the
690 TruSeq Stranded mRNA HT kit (Illumina, San Diego, CA) on an ePMotion 5075 robot
691 (Eppendorf, Hamburg, Germany). Libraries were uniquely barcoded, quantified, and pooled for
692 sequencing across 6 lanes with 100 nt single-end sequencing on the Illumina HiSeq 4000.

693 *ATACseq library preparation and sequencing*

694 The 500 µL tissue homogenate was additionally homogenized by aspirating through a 20
695 gauge needle followed by a 23 gauge needle 5 times each. Samples were centrifuged at 500g for
696 5 minutes at 4°C. Supernatant was removed, and cells were resuspended in 50 µL cold PBS+PIC.
697 15 µL of this cell suspension (approximately 1/10th of the total brain, ~100k cells) was placed into
698 a new microcentrifuge tube, and this was centrifuged at 500g for 5 minutes at 4°C as an additional
699 cell washing step. Supernatant was removed, and cells were gently resuspended in 50 µL cold lysis
700 buffer prepared as in Buenrostro et al. (2015). The remainder of the ATACseq library protocol
701 followed Buenrostro et al. (2015), with the exception of the final purification step, where a 0.8:1
702 ratio of Ampure XP beads (Beckman Coulter, Brea, CA) to sample was used to purify each library.
703 In addition to sample libraries, input libraries were constructed from thoracic genomic DNA from
704 a random bee from each colony per sequencing batch using 50 ng of genomic DNA (extracted
705 using the Gentra Puregene Tissue Kit from Qiagen, cat. #158667, following manufacturer's
706 protocol for DNA purification from 25 mg tissue but with 6 µL proteinase K and 4 µL RNase A
707 at the appropriate steps). Genomic DNA was transposed with Nextera Tn5 Transposase (Nextera
708 Kit, Illumina) following the ATACseq protocol immediately following the cell lysis step
709 (Buenrostro et al., 2015), again using an 0.8:1 Ampure XP bead clean-up at the end of the protocol.
710 A Qubit dsDNA HS Assay Kit (Invitrogen) was used to quantify each library, and library size and
711 quality was assessed using a Bioanalyzer High-Sensitivity DNA Analysis kit (Agilent).

712 ATACseq libraries, including input libraries, were pooled at equal nM concentrations and
713 a bead clean-up (0.8:1 ratio of Ampure XP beads to sample) was performed on the pool prior to
714 submission for sequencing. QC on the final pool was performed using qPCR and an AATI

715 Fragment Analyzer by the Keck Center. Libraries were sequenced across three lanes with 100 nt
716 paired-end sequencing on the Illumina HiSeq 4000 by the Keck Center.

717 *Data processing and analysis*

718 RNAseq

719 Sequencing of RNAseq libraries (n=45, 25 from colony E, 20 from colony F) produced
720 1,487,641,973 reads which survived quality and adapter trimming using Trimmomatic (version
721 0.36, parameters used: ILLUMINACLIP: 2:35:30 LEADING:20 TRAILING:20 MINLEN:30).
722 Trimmed reads were aligned to the *Apis mellifera* HAv3.1 genome (NCBI accession
723 GCA_003254395.2) using STAR (version 2.5.3) and default parameters, resulting in an average
724 of 96.7% reads mapping uniquely. The program featureCounts from the Subread package (version
725 1.5.2) was used to assign mapped reads to gene features from the GFF file from NCBI associated
726 with the *A. mellifera* HAv3.1 genome. On average, 84.8% of uniquely mapped reads were assigned
727 to gene features using featureCounts.

728 Gene counts were imported into R for differential expression analysis using edgeR. Genes
729 with less than 1 CPM in at least 2 samples were removed, and remaining count values were
730 normalized using the TMM method. Gene-wise variances were calculated by estimating tagwise
731 dispersions in edgeR on filtered gene count matrices for each group separately and plotted using
732 ggplot2. Tagwise dispersion estimates were followed by quasi-likelihood F-tests for each pairwise
733 comparison of groups, with FDR correction for multiple testing. Differentially expressed genes
734 (DEGs, FDR<0.05) for each pairwise comparison are given in Supplementary File 3.

735 ATACseq

736 ATACseq libraries (n=48, 25 from colony E, 20 from colony F, 3 input libraries) produced
737 1,110,401,018 paired-end reads which survived quality and adapter trimming using Trimmomatic
738 (version 0.38, parameters used: ILLUMINACLIP: 2:15:10 HEADCROP:10 LEADING:20
739 TRAILING 20 SLIDINGWINDOW:4:15 MINLEN:30). An average of 98.1% of reads mapped to
740 the *Apis mellifera* HAv3.1 genome using bwa mem (version 0.7.17, default parameters).
741 Duplicates were marked and removed prior to further processing using picard (version 2.10.1,
742 average duplication level 30.2%).

743 Peaks were called from deduplicated BAM files using MACS2 (version 2.1.1, command:
744 callpeak, with parameters: --nomodel -g 2.5e8 --nolambda --keep-dup all --slocal 10000) using the
745 appropriate colony and sequencing batch input as control. Peaks were called on each colony and

746 behavioral group separately, then merged and sorted using BEDTools (version 2.26.0, sort and
747 merge commands). This resulted in a total of 11,614 merged peaks with an average width of 721
748 bp. Mapped reads were counted to each peak per individual using featureCounts from the Subread
749 package (version 1.5.2). An average of 51.0% of reads were mapped to called peaks.

750 Peak counts were imported into R for differential accessibility analysis using edgeR. Peaks
751 with less than 1 CPM in at least 2 samples were removed, and remaining count values were
752 normalized using the TMM method. Gene-wise variances were calculated by estimating tagwise
753 dispersions in edgeR on filtered gene count matrices for each group separately and plotted using
754 ggplot2. Tagwise dispersion estimates were followed by quasi-likelihood F-tests for each pairwise
755 comparison of groups, with FDR correction for multiple testing. Differentially accessible peak
756 (DAP, FDR<0.05) results for each pairwise comparison are given in Supplementary File 4.

757 *Functional annotation of differential expression and chromatin accessibility*

758 Differential expression

759 Differentially expressed gene (DEG) lists were functionally annotated using Gene
760 Ontology (GO) by first mapping putative orthologs between *Apis mellifera* and *Drosophila*
761 *melanogaster* using reciprocal best BLASTP hits (e-value cutoff = 1e-5). Only DEGs with putative
762 *D. melanogaster* orthologs were included for GO enrichment, and the background list used was all
763 tested genes (those which passed the minimum expression threshold) with putative *D.*
764 *melanogaster* orthologs. Enrichment tests for biological processes were conducted using GOrilla
765 (Eden et al., 2009) with all significant DEGs (FDR<0.05) against the background list. GO
766 enrichment results for all DEG lists are given in Supplementary File 3.

767 Differential accessibility

768 To functionally annotate DAPs, the midpoint coordinate of the 11,614 peaks identified with
769 MACS2 were assigned to genes based on proximity to honey bee gene features (*Apis mellifera*
770 HAv3.1 genome). The following features were considered per gene: promoters (1 kb upstream),
771 introns, exons, 5' UTR, 3' UTR, upstream (10 kb upstream), and downstream (10 kb). Peaks not
772 associated with any gene feature were classified as intergenic. When peaks were associated with
773 multiple genes (e.g., the intron of one gene and the promoter of another), they were assigned to
774 individual genes based on the following priority: promoter (highest priority), exon, 5' UTR, 3'
775 UTR, intron, upstream, downstream (lowest priority). If a peak was present in the same highest
776 priority class for multiple genes, it was randomly assigned to one gene. In this way, each peak was

assigned to either a single gene or considered intergenic. Of the 11,614 peaks, 1822 were assigned to the promoter region of a gene, 776 to exons, 1326 to 5' UTRs, 273 to 3' UTRs, 4666 to introns, 1155 to upstream regions, 773 to downstream regions, and 823 peaks were located in intergenic regions.

As before with GO enrichment for DEGs, differentially accessible peaks (DAPs) were functionally annotated by mapping peak-associated genes to putative orthologs in *D. melanogaster* using BLASTP. The background list for enrichment analyses was the list of peaks which met the minimum accessibility count threshold for analysis and which had putative orthologs in *D. melanogaster.* GOrilla (Eden et al., 2009) was used for enrichment tests. GO enrichment results for all DAP lists are given in Supplementary File 4.

Motif enrichment of DAPs and DEG regulatory regions

Transcription factor (TF) motif enrichment analysis in this study was performed similarly to the methods described in Whitney et al. (2014). The overall approach is as follows, with details below. For each TF motif, 1) genomic windows were scored for the presence of the motif, 2) window scores were combined into scores for genomic segments of interest, representing either gene regulatory regions or accessibility peaks, 3) a set of motif targets was created using a fixed cutoff on the segment scores, and 4) a statistical test for enrichment was performed between segments that were motif targets and those that were significant in differential analysis.

<u>Motif scores for genomic windows</u>

First, we divided the honey bee genome (version HAv3.1, NCBI accession GCA_003254395.2) into 500 bp windows with 250 bp shifts. We gathered a collection of 223 representative TFs (Kapheim et al., 2015) and downloaded their DNA binding specificities (motifs) characterized as position weight matrices (PWMs) from FlyFactorSurvey (Zhu et al., 2011). Separately for each TF motif, we ran the Stubb algorithm (Sinha et al., 2003) on all genomic windows to score them for the presence of that TF's binding sites. Tandem repeats in the windows were masked using the Tandem Repeat Finder (Benson, 1999) before calculating the Stubb scores to avoid scoring the repeats as weak binding sites. Since the honey bee genome has significant local G/C heterogeneity (Sinha et al., 2006), we converted the raw Stubb scores for each window into G/C content-normalized empirical p-values. This was done by determining the rank of each window among all genomic windows of similar G/C content (when grouped into 20 G/C bins).

807 Scores for genomic segments

808 We defined two different collections of genomic segments (accessibility peaks and gene
809 regulatory regions) to analyze with motif enrichment in this study. Since the genomic segments
810 may overlap with a variable number of our genomic windows, we defined a length-adjusted motif
811 score for each segment. This score was calculated using the score of the best scoring window in
812 that segment for the given motif and the number of windows overlapping the segment, as follows:

813 $$sc_{seg} = 1 - (1 - pval_{best})^N$$

814 where sc_{seg} = length-adjusted motif score for the segment, N = number of windows that overlap
815 with the scoring window, and $pval_{best}$ = best G/C normalized empirical p-value among the N
816 overlapping windows.

817 Statistical test for TF enrichment

818 TF enrichment was analyzed for two sets of regions: DAPs (Differentially Accessible
819 Peaks) and DEGs (Differentially Expressed Genes) (Supplementary File 7).

820 For analysis of DAPs, the collection of genomic segments was defined as the combination
821 of all DAPs and randomly selected non-accessible parts of genome that had the same distribution
822 of lengths as those DAPs. The number of randomly selected genomic segments was set to 10 times
823 the number of DAP segments. For each motif, the top 200 scoring segments from the collection
824 were defined as the TF motif target set. Hypergeometric p-values were calculated for each motif-
825 DAP set pair (Supplementary File 7) to quantify the significance of the overlap between the
826 corresponding TF motif target set and DAP set.

827 For DEGs, the collection of genomic segments was the regulatory regions of all genes in
828 the honey bee annotation. Each regulatory region was defined as 5kb upstream to 2kb downstream
829 of the transcriptional start site of its gene (http://veda.cs.uiuc.edu/beeMotifScores/). The top 500
830 scoring segments from the gene universe were selected as the TF motif target set for each motif.
831 Finally, the significance of the overlap for each motif-DEG set pair (Supplementary File 7) was
832 calculated with the Hypergeometric p-value.

833 All p-values were then converted to q-values using the "qvalue" function in the R software
834 package qvalue (Storey et al., 2019) to control the false discovery rate from multiple hypothesis
835 testing.

836 For motifs enriched both within DAPs and DEG upstream regions, CentriMo (Bailey and
837 Machanick, 2012) from MEME Suite was used to calculate and plot the probability of motif
838 binding across 2 kb windows centered on the peak summit for DAPs and 7 kb windows (5kb
839 upstream and 2kb downstream of the transcriptional start site (TSS)) for DEGs. These probabilities
840 are shown in Fig. 3B-C.

841 *Individualized Gene Regulatory Network (GRN) analysis*

842 To understand how TFs orchestrate transcriptional changes in the brain, we reconstructed
843 a gene regulatory network (GRN) model using the ASTRIX approach (Chandrasekaran, 2014;
844 Chandrasekaran et al., 2011). ASTRIX uses gene expression data to identify interactions between
845 TFs and their target genes. The ASTRIX algorithm has been previously used to infer brain GRN
846 models for various organisms including the honey bee (Bukhari et al., 2017; Saul et al., 2017;
847 Shpigler et al., 2017). These models showed significantly high accuracy in predicting gene
848 expression changes in the brain and identified TFs that regulate social behaviors.

849 Here we applied ASTRIX using the gene expression data of the 45 individual bees along
850 with a list of honey bee TFs as input to identify regulatory interactions. We normalized the
851 transcriptomics data prior to GRN construction using the ComBat algorithm (Johnson et al., 2007)
852 to minimize batch and colony effects in the data. The effectiveness of the normalization was
853 checked using PCA. Any TF predicted to interact with a given target gene by ASTRIX had to pass
854 through two criteria: 1) share a significant degree of mutual information with the target gene (p-
855 value $< 10^{-6}$), and 2) explain at least 10% of the variance of the target gene, quantified by Least
856 angle regression algorithm. Similarly, each target gene included in the GRN must be predicted
857 with a correlation of at least 0.8 by the ASTRIX model using expression levels of TFs.

858 The GRN model built by ASTRIX predicted 2,190 genes with a Pearson's correlation of
859 0.8 or higher using expression levels of TFs. Overall, the GRN inferred by ASTRIX contains 4,500
860 interactions between 190 TFs and the 2,190 target genes. The full GRN is in Supplementary File
861 8.

862 To determine TFs correlated with specific behaviors, we first identified genes that were
863 strongly correlated with specific behavior scores across all individuals (FDR p-value of correlation
864 < 0.001). TFs whose targets were over-represented among the behavior-correlated genes were then
865 determined. Significance of the overlap between the list of behavior-correlated genes with targets
866 of each TF ("TF module") was estimated using the hypergeometric test.

867 Finally, to identify TF modules associated with expression changes in each individual
868 ("Individualized TF modules"), genes that were upregulated or downregulated in each individual
869 were identified using z-transformation. Genes in each individual with z-scores above 2 (i.e., 2
870 standard deviations above mean) or below -2 were considered to be differentially expressed in an
871 individual. This list of genes was then overlapped with TF modules to identify modules
872 significantly associated with each individual using the hypergeometric test of overlap.

873 We used a Random Forests classification algorithm for predicting individual behavioral
874 group from TF expression levels. A leave-one-out cross validation analysis was performed wherein
875 the algorithm was trained using data from the remaining 44 individuals and then used to predict
876 the behavior of the 45th individual using its TF levels. The model achieved an accuracy of 82% in
877 predicting behavior. Performance of the model was evaluated by comparison with random
878 shuffling of the behavior labels. We made predictions 100 times with a different set of shuffled
879 labels and compared the accuracy of predictions (i.e., total individuals for which behavioral group
880 was correctly predicted) between the random model and the Random Forest algorithm using a t-
881 test ($p=1 \times 10^{-8}$). This suggests that TF expression levels can accurately forecast the behavior of
882 the individual, especially for specialists. The relative importance of each TF in predicting behavior
883 was determined using Out-of-bag predictor importance estimation, wherein each predictor's value
884 is permuted and the corresponding impact on model accuracy is determined (importance scores
885 given in Supplementary File 8). The random forest classification algorithm was implemented in
886 MATLAB with default parameters for the number of predictors sampled (square root of the
887 number of predictors, in this case 258 TFs) and default values for the tree depth (n - 1, where n is
888 the training data size).

889 *Selection of candidate TFs involved in specialized phenotypes*

890 Candidate TFs displayed in Fig. 5 were drawn from multiple analyses presented in this
891 paper and in Kapheim et al. (2015). "Enriched within DAPs" indicates enrichment of the TF motif
892 within forager vs. layer DAPs from the analysis of ATACseq data within this manuscript (see
893 *Motif enrichment of DAPs and DEG promoters* and Supplementary File 7*)*. Similarly, "Enriched
894 near DEGs" indicates enrichment of the TF motif among putative regulatory regions of forager vs.
895 layer DEGs (see *Motif enrichment of DAPs and DEG promoters* and Supplementary File 7*)*.
896 "Module correlated with behavior" indicates that TF module activity is significantly correlated
897 with at least one behavioral metric across individuals (see *Individualized Gene Regulatory*

898 *Network (GRN) analysis* and Supplementary File 8). "Group Predictive TF" indicates the TF is
899 among the 20 most informative for predicting individual group membership based on TF
900 expression (see *Individualized Gene Regulatory Network (GRN) analysis* and Supplementary File
901 8). "Implicated in eusocial evolution" indicates that the TF motif was previously found to be
902 associated with social evolution in Kapheim et al. (2015).
903
904 **Acknowledgements**
905 We thank A. Sankey, A. Ray, S. Bransley, J. Cullum, K. Wilk and J. Falk for assistance
906 in the field, A. Hernandez and the staff at the Carver Biotechnology Center for sequencing
907 services, administrators of Biocluster (UIUC) for computational support, and M.B. Sokolowski,
908 M. Hudson, A.M. Bell, members of the Robinson lab, and three anonymous reviewers for
909 comments that improved this manuscript. Funding: This research was supported by Grant
910 R01GM117467 from the National Institute of General Medical Sciences (GER and N.
911 Goldenfeld, PIs), the Christopher Foundation (GER), and the Illinois Sociogenomics Initiative
912 (GER). Data and materials availability: The raw sequence data reported in this paper have been
913 deposited at the National Center for Biotechnology Information (NCBI) Sequence Read Archive,
914 Accession PRJNA593999. Requests for materials should be addressed to B.M.J.
915
916 **Competing interests**
917 No competing interests declared.
918
919 **References**
920 Abadi M, Barham P, Chen J, Chen Z, Davis A, Dean J, Devin M, Ghemawat S, Irving G, Isard
921 M, Kudlur M, Levenberg J, Monga R, Moore S, Murray DG, Steiner B, Tucker P,
922 Vasudevan V, Warden P, Wicke M, Yu Y, Zheng X, Brain G, Osdi I, Barham P, Chen J,
923 Chen Z, Davis A, Dean J, Devin M, Ghemawat S, Irving G, Isard M, Kudlur M, Levenberg
924 J, Monga R, Moore S, Murray DG, Steiner B, Tucker P, Vasudevan V, Warden P, Wicke
925 M, Yu Y, Zheng X. 2016. TensorFlow : A system for large-scale machine learning. *OSDI*
926 **16**:265–283. doi:10.1126/science.aab4113.4
927 Adams J, Rothman ED, Kerr WE, Paulino ZL. 1977. Estimation of the number of sex alleles and
928 queen matings from diploid male frequencies in a population of *Apis mellifera*. *Genetics*

929 **86**:583–596.
930 Alaux C, Le Conte Y, Adams HA, Rodriguez-Zas S, Grozinger CM, Sinha S, Robinson GE.
931 2009. Regulation of brain gene expression in honey bees by brood pheromone. *Genes,*
932 *Brain Behav* **8**:309–319. doi:10.1111/j.1601-183X.2009.00480.x
933 Ament S, Wang Y, Chen C-C, Blatti C, Hong F, Liang Z, Negre N, White K, Rodriquez-Zas S,
934 Mizzen C, Zinha S, Zhong S, Robinson G. 2012. The transcription factor *ultraspiracle*
935 influences honey bee social behavior and behavior-related gene expression. *PLoS Genet*
936 **8**:e1002596. doi:10.1371/journal.pgen.1002596
937 Araya CL, Kawli T, Kundaje A, Jiang L, Wu B, Vafeados D, Terrell R, Weissdepp P,
938 Gevirtzman L, Mace D, Niu W, Boyle AP, Xie D, Ma L, Murray JI, Reinke V, Waterston
939 RH, Snyder M. 2014. Regulatory analysis of the *C. elegans* genome with spatiotemporal
940 resolution. *Nature* **512**:400–405. doi:10.1038/nature16075
941 Bailey TL, Machanick P. 2012. Inferring direct DNA binding from ChIP-seq. *Nucleic Acids Res*
942 **40**:e128.
943 Barth RH, Lester LJ, Sroka P, Kessler T, Hearn R. 1975. Juvenile hormone promotes dominance
944 behavior and ovarian development in social wasps (*Polistes annularis*). *Experientia*
945 **31**:691–692. doi:10.1007/BF01944632
946 Benson G. 1999. Tandem repeats finder: A program to analyze DNA sequences. *Nucleic Acids*
947 *Res*. doi:10.1093/nar/27.2.573
948 Branstetter MG, Danforth BN, Pitts JP, Faircloth BC, Ward PS, Buffington ML, Gates MW,
949 Kula RR, Brady SG. 2017. Phylogenomic insights into the evolution of stinging wasps and
950 the origins of ants and bees. *Curr Biol* **27**:1019–1025. doi:10.1016/j.cub.2017.03.027
951 Buenrostro J, Giresi P, Zaba L, Chang H, Greenleaf W. 2013. Transposition of native chromatin
952 for fast and sensitive epigenomic profiling of open chromatin, DNA-binding proteins and
953 nucleosome position. *Nat Methods* **10**:1213–1218.
954 Buenrostro JD, Wu B, Chang HY, Greenleaf WJ. 2015. ATAC-seq: A Method for Assaying
955 Chromatin Accessibility Genome-Wide. *Curr Protoc Mol Biol* **109**:21.29.1-21.29.9.
956 Bukhari SA, Saul MC, James N, Bensky MK, Stein LR, Trapp R, Bell AM. 2019. Neurogenomic
957 insights into paternal care and its relation to territorial aggression. *Nat Commun* **10**:4437.
958 doi:10.1038/s41467-019-12212-7
959 Bukhari SA, Saul MC, Seward CH, Zhang H, Bensky M, James N, Zhao SD, Chandrasekaran S,

960 Stubbs L, Bell AM. 2017. Temporal dynamics of neurogenomic plasticity in response to
961 social interactions in male threespined sticklebacks. *PLoS Genet* **13**:e1006840.
962 doi:10.1371/journal.pgen.1006840
963 Chan YF, Marks ME, Jones FC, Villarreal G, Shapiro MD, Brady SD, Southwick AM, Absher
964 DM, Grimwood J, Schmutz J, Myers RM, Petrov D, Jónsson B, Schluter D, Bell MA,
965 Kingsley DM. 2010. Adaptive evolution of pelvic reduction in sticklebacks by recurrent
966 deletion of a *Pitxl* enhancer. *Science* **327**:302–5. doi:10.1126/science.1182213
967 Chandrasekaran S, Ament SA, Eddy JA, Rodriguez-Zas SL, Schatz BR, Price ND, Robinson GE.
968 2011. Behavior-specific changes in transcriptional modules lead to distinct and predictable
969 neurogenomic states. *Proc Natl Acad Sci* **108**:18020.
970 Chandrasekaran S. 2014. Predicting phenotype from genotype through reconstruction and
971 integrative modeling of metabolic and regulatory networksA Systems Theoretic Approach
972 to Systems and Synthetic Biology I: Models and System Characterizations. pp. 307–325.
973 doi:10.1007/978-94-017-9041-3_12
974 Cnaani J, Schmid-Hempel R, Schmidt JO. 2002. Colony development, larval development and
975 worker reproduction in *Bombus impatiens* Cresson. *Insectes Soc* **49**:164–170.
976 doi:10.1007/s00040-002-8297-8
977 Crall JD, Gravish N, Mountcastle AM, Combes SA. 2015. BEEtag: A low-cost, image-based
978 tracking system for the study of animal behavior and locomotion. *PLoS One* **10**:e0136487.
979 doi:10.1371/journal.pone.0136487
980 Cummings ME, Larkins-Ford J, Reilly CRL, Wong RY, Ramsey M, Hofmann HA. 2008. Sexual
981 and social stimuli elicit rapid and contrasting genomic responses. *Proc R Soc B Biol Sci*
982 **275**:393–402. doi:10.1098/rspb.2007.1454
983 Dadant & Sons. 1975. Activities of queenless bees In: Dadant & Sons, editor. The Hive and the
984 Honey Bee. Carthage, Illinois: Journal Printing Company. pp. 245–247.
985 Dornhaus A. 2008. Specialization does not predict individual efficiency in an ant. *PLoS Biol*
986 **6**:2368–2375. doi:10.1371/journal.pbio.0060285
987 Dufour HD, Koshikawa S, Finet C. 2020. Temporal flexibility of gene regulatory network
988 underlies a novel wing pattern in flies. *Proc Natl Acad Sci U S A* **117**:11589–11596.
989 doi:10.1073/pnas.2002092117
990 Eden E, Navon R, Steinfeld I, Lipson D, Yakhini Z. 2009. GOrilla: A tool for discovery and

991 visualization of enriched GO terms in ranked gene lists. *BMC Bioinformatics* **10**:48.
992 doi:10.1186/1471-2105-10-48
993 Estoup A, Solignac M, Cornuet JM. 1994. Precise assessment of the number of patrilines and of
994 genetic relatedness in honeybee colonies. *Proc R Soc B Biol Sci* **258**:1–7.
995 doi:10.1098/rspb.1994.0133
996 Fine JD, Shpigler HY, Ray AM, Beach NJ, Sankey AL, Cash-Ahmed A, Huang ZY,
997 Astrauskaite I, Chao R, Zhao H, Robinson GE. 2018. Quantifying the effects of pollen
998 nutrition on honey bee queen egg laying with a new laboratory system. *PLoS One*
999 **13**:e0203444. doi:10.1371/journal.pone.0203444
1000 FlyBase Consortium, Thurmond J, Goodman JL, Strelets VB, Attrill H, Gramates LS, Marygold
1001 SJ, Matthews BB, Millburn G, Antonazzo G, Trovisco V, Kaufman TC, Calvi BR. 2019.
1002 FlyBase 2.0: the next generation. *Nucleic Acids Research* **47**:D759-D765.
1003 doi:10.1093/nar/gky1003
1004 Free JB. 1955. The behaviour of egg-laying workers of bumblebee colonies. *Br J Anim Behav*
1005 **3**:147–153. doi:10.1016/S0950-5601(55)80053-6
1006 Gadagkar R. 1997. The evolution of caste polymorphism in social insects genetic release
1007 followed by diversifying evolution. *J Genet* **76**:167–179. doi:10.1007/BF02932215
1008 Geffre AC, Gernat T, Harwood GP, Jones BM, Gysi DM, Hamilton AR, Bonning BC, Toth AL,
1009 Robinson GE, Dolezal AG. 2020. Honey bee virus causes context-dependent changes in
1010 host social behavior. *Proc Natl Acad Sci U S A*. doi:10.1073/pnas.2002268117
1011 Gençer HV, Kahya Y. 2011. Are sperm traits of drones (*Apis mellifera* L.) from laying worker
1012 colonies noteworthy? *J Apic Res* **50**:130–137. doi:10.3896/IBRA.1.50.2.04
1013 Gernat T, Rao VD, Middendorf M, Dankowicz H, Goldenfeld N, Robinson GE. 2018.
1014 Automated monitoring of behavior reveals bursty interaction patterns and rapid spreading
1015 dynamics in honeybee social networks. *Proc Natl Acad Sci* **115**:1433–1438.
1016 doi:10.1073/pnas.1713568115
1017 Gernat T, Jagla T, Jones BM, Middendorf M, Robinson GE. 2020. Automated monitoring of
1018 animal behaviour with barcodes and convolutional neural networks. *bioRxiv.*
1019 doi:10.1101/2020.11.27.401760
1020 Graham AM, Munday MD, Kaftanoglu O, Page RE, Amdam G V., Rueppell O. 2011. Support
1021 for the reproductive ground plan hypothesis of social evolution and major QTL for ovary

1022 traits of Africanized worker honey bees (*Apis mellifera* L.). *BMC Evol Biol* **11**:95.
1023 doi:10.1186/1471-2148-11-95
1024 Greenwald E, Segre E, Feinerman O. 2015. Ant trophallactic networks: simultaneous
1025 measurement of interaction patterns and food dissemination. *Sci Rep* **5**:12496.
1026 Grozinger CM, Fan Y, Hoover SER, Winston ML. 2007. Genome-wide analysis reveals
1027 differences in brain gene expression patterns associated with caste and reproductive status
1028 in honey bees (*Apis mellifera*). *Mol Ecol* **16**:4837–4848.
1029 Hamilton AR, Shpigler H, Bloch G, Wheeler DE, Robinson GE. 2016. Endocrine Influences on
1030 Insect Societies.Hormones, Brain and Behavior: Third Edition. doi:10.1016/B978-0-12-
1031 803592-4.00037-7
1032 Hamilton AR, Traniello IM, Ray AM, Caldwell AS, Wickline SA, Robinson GE. 2019. Division
1033 of labor in honey bees is associated with transcriptional regulatory plasticity in the brain. *J*
1034 *Exp Biol* **222**:jeb200196. doi:10.1242/jeb.200196
1035 Harpur BA, Kent CF, Molodtsova D, Lebon JM, Alqarni AS, Owayss AA, Zayed A. 2014.
1036 Population genomics of the honey bee reveals strong signatures of positive selection on
1037 worker traits. *Proc Natl Acad Sci* **111**:2614–2619.
1038 Hess G. 1942. Über den einfluss der weisellosigkeit und des fruchtbarkeitsvitamins e auf die
1039 ovarien der bienenarbeiterin. *Schweiz Bienen Ztg* **2**:33–110.
1040 Holldobler B, Wilson EO. 1990. The Ants. Cambridge, MA: Belknap/Harvard Univ. Press.
1041 Jeanson R, Clark RM, Holbrook CT, Bertram SM, Fewell JH, Kukuk PF. 2008. Division of
1042 labour and socially induced changes in response thresholds in associations of solitary
1043 halictine bees. *Anim Behav* **76**:593–602. doi:10.1016/j.anbehav.2008.04.007
1044 Johnson WE, Li C, Rabinovic A. 2007. Adjusting batch effects in microarray expression data
1045 using empirical Bayes methods. *Biostatistics* **8**:118–127. doi:10.1093/biostatistics/kxj037
1046 Jones BM, Kingwell CJ, Wcislo WT, Robinson GE. 2017. Caste-biased gene expression in a
1047 facultatively eusocial bee suggests a role for genetic accommodation in the evolution of
1048 eusociality. *Proc R Soc B Biol Sci* **284**:20162228.
1049 Kapheim KM, Jones BM, Pan H, Li C, Harpur BA, Kent CF, Zayed A, Ioannidis P, Waterhouse
1050 RM, Kingwell C, Stolle E, Avalos A, Zhang G, McMillan WO, Wcislo WT. 2020.
1051 Developmental plasticity shapes social traits and selection in a facultatively eusocial bee.
1052 *Proc Natl Acad Sci U S A* **117**:13615–13625. doi:10.1073/pnas.2000344117

1053 Kapheim KM, Pan H, Li C, Salzberg SL, Puiu D, Magoc T, Robertson HM, Hudson ME, Venkat
1054 A, Fischman BJ, Hernandez A, Yandell M, Ence D, Holt C, Yocum GD, Kemp WP, Bosch
1055 J, Waterhouse RM, Zdobnov EM, Stolle E, Kraus FB, Helbing S, Moritz RFA, Glastad KM,
1056 Hunt BG, Goodisman MAD, Hauser F, Grimmelikhuijzen CJP, Pinheiro DG, Nunes FMF,
1057 Soares MPM, Tanaka ÉD, Simões ZLP, Hartfelder K, Evans JD, Barribeau SM, Johnson
1058 RM, Massey JH, Southey BR, Hasselmann M, Hamacher D, Biewer M, Kent CF, Zayed A,
1059 Blatti C, Sinha S, Johnston JS, Hanrahan SJ, Kocher SD, Wang J, Robinson GE, Zhang G.
1060 2015. Genomic signatures of evolutionary transitions from solitary to group living. *Science*
1061 **348**:1139–1143.
1062 Lobo J, Kerr W. 1993. Estimation of the number of matings in *Apis mellifera*: extensions of the
1063 model and comparison of different estimates. *Ethol Ecol Evol* **5**:337–345.
1064 Mallarino R, Campàs O, Fritz JA, Burns KJ, Weeks OG, Brenner MP, Abzhanov A. 2012.
1065 Closely related bird species demonstrate flexibility between beak morphology and
1066 underlying developmental programs. *Proc Natl Acad Sci U S A* **109**:16222–16227.
1067 doi:10.1073/pnas.1206205109
1068 Mello C V, Vicario DS, Clayton DF. 1992. Song presentation induces gene expression in the
1069 songbird forebrain. *Proc Natl Acad Sci U S A* **89**:6818–6822. doi:10.1073/pnas.89.15.6818
1070 Mersch DP, Crespi A, Keller L. 2013. Tracking individuals shows spatial fidelity is a key
1071 regulator of ant social organization. *Science* **340**:1090. doi:10.1126/science.1234316
1072 Michener CD. 1974. The Social Behavior of the Bees: A Comparative Study. Cambridge, MA:
1073 Harvard University Press.
1074 Miller III DG, Ratnieks FLW. 2001. The timing of worker reproduction and breakdown of
1075 policing behaviour in queenless honey bee (*Apis mellifera* L.) societies. *Insectes Soc*
1076 **48**:178.
1077 Morse RA. 1990. Laying workers In: Morse RA, Flottum K, editors. The ABC & XYZ of Bee
1078 Culture. The A. I. Root Company. pp. 291–293.
1079 Mukherjee D, Ignatowska-Jankowska BM, Itskovits E, Gonzales BJ, Turm H, Izakson L, Haritan
1080 D, Bleistein N, Cohen C, Amit I, Shay T, Grueter B, Zaslaver A, Citri A. 2018. Salient
1081 experiences are represented by unique transcriptional signatures in the mouse brain. *Elife*
1082 **7**:e31220. doi:10.7554/eLife.31220
1083 Naeger NL, Peso M, Even N, Barron AB, Robinson GE. 2013. Altruistic behavior by egg-laying

1084 worker honeybees. *Curr Biol* **23**:1574–1578. doi:10.1016/j.cub.2013.06.045
1085 O'Donnell S. 1998. Reproductive caste determination in eusocial wasps (Hymenoptera:
1086 Vespidae). *Annu Rev Entomol* **43**:323–346. doi:10.1146/annurev.ento.43.1.323
1087 Oster GF, Wilson EO. 1979. Caste and Ecology in the Social Insects. Princeton: Princeton
1088 University Press. doi:10.1007/s00265-010-1009-x
1089 Page RE, Rueppell O, Amdam G V. 2012. Genetics of reproduction and regulation of honey bee
1090 (*Apis mellifera* L.) social behavior. *Annu Rev Genet* **46**:19–97.
1091 Page RE, Erickson EH. 1988. Reproduction by worker honey bees (Apis mellifera). *Behav Ecol*
1092 *Sociobiol* **23**:117–126. doi:10.1007/BF00299895
1093 Page RE, Robinson GE. 1991. The Genetics of Division of Labour in Honey Bee Colonies. *Adv*
1094 *In Insect Phys* **23**:118–169. doi:10.1016/S0065-2806(08)60093-4
1095 Page RE, Robinson GE. 1994. Reproductive competition in queenless honey bee colonies (*Apis*
1096 *mellifera* L.). *Behav Ecol Sociobiol* **35**:99–107. doi:10.1007/BF00171499
1097 Prud'homme B, Gompel N, Rokas A, Kassner VA, Williams TM, Yeh SD, True JR, Carroll SB.
1098 2006. Repeated morphological evolution through *cis*-regulatory changes in a pleiotropic
1099 gene. *Nature* **440**:1050–3. doi:10.1038/nature04597
1100 Ratnieks FW. 1993. Egg-laying, egg-removal, and ovary development by workers in queenright
1101 honey bee colonies. *Behav Ecol and Sociobiol* **32**:191-198.
1102 Ratnieks FLW, Foster KR, Wenseleers T. 2006. Conflict resolution in insect societies. *Annu Rev*
1103 *Entomol* **51**:581–608. doi:10.1146/annurev.ento.51.110104.151003
1104 Ratnieks FLW, Wenseleers T. 2008. Altruism in insect societies and beyond: voluntary or
1105 enforced? *Trends Ecol Evol* **23**:45–52. doi:10.1016/j.tree.2007.09.013
1106 Reed RD, Papa R, Martin A, Hines HM, Counterman BA, Pardo-Diaz C, Jiggins CD,
1107 Chamberlain NL, Kronforst MR, Chen R, Halder G, Nijhout HF, McMillan WO. 2011.
1108 *Optix* drives the repeated convergent evolution of butterfly wing pattern mimicry. *Science*
1109 **333**:1137.
1110 Rittschof CC, Bukhari SA, Sloofman LG, Troy JM, Caetano-Anollés D, Cash-Ahmed A, Kent
1111 M, Lu X, Sanogo YO, Weisner PA, Zhang H, Bell AM, Ma J, Sinha S, Robinson GE,
1112 Stubbs L. 2014. Neuromolecular responses to social challenge: Common mechanisms
1113 across mouse, stickleback fish, and honey bee. *Proc Natl Acad Sci* **111**:17929–17934.
1114 Robinson GE, Page RE, Fondrk MK. 1990. Intracolonial behavioral variation in worker

1115 oviposition, oophagy, and larval care in queenless honey bee colonies. *Behav Ecol*
1116 *Sociobiol* **26**:315–323. doi:10.1007/BF00171096
1117 Robinson GE. 1992. Regulation of division of labor in insect societies. *Annu Rev Entomol*
1118 **37**:637–665.
1119 Robinson GE, Strambi C, Strambi A, Huang ZY. 1992. Reproduction in worker honey bees is
1120 associated with low juvenile hormone titers and rates of biosynthesis. *Gen Comp*
1121 *Endocrinol* **87**:471–480. doi:10.1016/0016-6480(92)90055-O
1122 Sakagami SF. 1954. Occurrence of an aggressive behaviour in queenless hives, with
1123 considerations on the social organization of honeybee. *Insectes Soc* **1**:331–343.
1124 doi:10.1007/BF02329618
1125 Saul MC, Seward CH, Troy JM, Zhang H, Sloofman LG, Lu X, Weisner PA, Caetano-Anolles
1126 D, Sun H, Zhao SD, Chandrasekaran S, Sinha S, Stubbs L. 2017. Transcriptional regulatory
1127 dynamics drive coordinated metabolic and neural response to social challenge in mice.
1128 *Genome Res* **27**:959–972. doi:10.1101/gr.214221.116
1129 Schindelin J, Arganda-Carreras I, Frise E, Kaynig V, Longair M, Pietzsch T, Preibisch S,
1130 Rueden C, Saalfeld S, Schmid B, Tinevez JY, White DJ, Hartenstein V, Eliceiri K,
1131 Tomancak P, Cardona A. 2012. Fiji: An open-source platform for biological-image
1132 analysis. *Nat Methods* **9**:676. doi:10.1038/nmeth.2019
1133 Schulz DJ, Robinson GE. 1999. Biogenic amines and division of labor in honey bee colonies:
1134 Behaviorally related changes in the antennal lobes and age-related changes in the mushroom
1135 bodies. *J Comp Physiol A* **184**:481–488. doi:10.1007/s003590050348
1136 Seeley TD. 2009. The Wisdom of the Hive: the social physiology of honey bee colonies,
1137 Proceedings of the Royal Society B: Biological Sciences. doi:10.1098/rspb.2010.0491
1138 Shpigler HY, Saul MC, Murdoch EE, Cash-Ahmed AC, Seward CH, Sloofman L,
1139 Chandrasekaran S, Sinha S, Stubbs LJ, Robinson GE. 2017. Behavioral, transcriptomic and
1140 epigenetic responses to social challenge in honey bees. *Genes, Brain Behav* **16**:579–591.
1141 doi:10.1111/gbb.12379
1142 Simola DF, Graham RJ, Brady CM, Enzmann BL, Desplan C, Ray A, Zwiebel LJ, Bonasio R,
1143 Reinberg D, Liebig J, Berger SL. 2015. Epigenetic (re)programming of caste-specific
1144 behavior in the ant *Camponotus floridanus*. *Science* **351**:aac6633.
1145 Sinha S, van Nimwegen E, Siggia ED. 2003. A probabilistic method to detect regulatory

1146 modules. *Bioinformatics* **19 Suppl 1**:i292-301. doi:10.1093/bioinformatics/btg1040
1147 Sinha S, Ling X, Whitfield CW, Zhai C, Robinson GE. 2006. Genome scan for *cis*-regulatory
1148 DNA motifs associated with social behavior in honey bees. *Proc Natl Acad Sci U S A*
1149 **103**:16352–16357. doi:10.1073/pnas.0607448103
1150 Sinha S, Jones BM, Traniello IM, Bukhari SA, Halfon MS, Hofmann HA, Huang S, Katz PS,
1151 Keagy J, Lynch VJ, Sokolowski MB, Stubbs LJ, Tabe-Bordbar S, Wolfner MF, Robinson
1152 GE. 2020. Behavior-related gene regulatory networks: A new level of organization in the
1153 brain. *Proc Natl Acad Sci U S A*. doi:10.1073/pnas.1921625117
1154 Storey JD, Bass AJ, Dabney A, Robinson D. 2019. qvalue: Q-value estimation for false
1155 discovery rate control. R package version 2.14.1.
1156 Toth AL, Várala K, Henshaw MT, Rodriguez-Zas SL, Hudson ME, Robinson GE. 2010. Brain
1157 transcriptomic analysis in paper wasps identifies genes associated with behaviour across
1158 social insect lineages. *Proc R Soc B Biol Sci* **277**:2139–2148. doi:10.1098/rspb.2010.0090
1159 Trumbo ST, Robinson GE. 1997. Learning and task interference by corpse-removal specialists in
1160 honey bee colonies. *Ethology* **103**:966–975. doi:10.1111/j.1439-0310.1997.tb00138.x
1161 Tsuruda JM, Amdam GV, Page RE. 2008. Sensory response system of social behavior tied to
1162 female reproductive traits. *PLoS One* **3**:e3397.
1163 Turillazzi S, West-Eberhard M. 1996. Natural History and Evolution of Paper-Wasps. Oxford:
1164 Oxford University Press.
1165 Velthuis HHW. 1970. Ovarian development in *Apis mellifera* worker bees. *Entomol Exp Appl*
1166 **13**:377.
1167 Velthuis HHW, Duchateau MJ. 2011. Ovarian development and egg laying in workers of
1168 *Bombus terrestris*. *Entomol Exp Appl* **51**:199–213.
1169 Visscher PK. 1996. Reproductive conflict in honey bees: a stalemate of worker egg-laying and
1170 policing. *Behav Ecol Sociobiol* **39**:237-244.
1171 Wario F, Wild B, Couvillon MJ, Rojas R, Landgraf T. 2015. Automatic methods for long-term
1172 tracking and the detection and decoding of communication dances in honeybees. *Front Ecol*
1173 *Evol* **3**:103. doi:10.3389/fevo.2015.00103
1174 Wenseleers T, Ratnieks FLW. 2006. Enforced altruism in insect societies. *Nature* **444**:50.
1175 doi:10.1038/444050a
1176 Werner T, Koshikawa S, Williams TM, Carroll SB. 2010. Generation of a novel wing colour

1177 pattern by the Wingless morphogen. *Nature* **464**:1143–1148. doi:10.1038/nature08896
1178 West-Eberhard MJ. 1987. Flexible strategy and social evolution, Animal societies: theories and
1179 facts. Tokyo: Japan Scientific Societies Press.
1180 Wheeler DE. 1986. Developmental and physiological determinants of caste in social
1181 Hymenoptera: Evolutionary implications. *Am Nat* **128**:13–34.
1182 Wheeler MM, Ament SA, Rodriguez-Zas SL, Robinson GE. 2013. Brain gene expression
1183 changes elicited by peripheral vitellogenin knockdown in the honey bee. *Insect Mol Biol*
1184 **22**:562–573.
1185 Whitfield CW, Cziko AM, Robinson GE. 2003. Gene expression profiles in the brain predict
1186 behavior in individual honey bees. *Science* **302**:296–299. doi:10.1126/science.1086807
1187 Whitney O, Pfenning AR, Howard JT, Blatti CA, Liu F, Ward JM, Wang R, Audet JN, Kellis M,
1188 Mukherjee S, Sinha S, Hartemink AJ, West AE, Jarvis ED. 2014. Core and region-enriched
1189 networks of behaviorally regulated genes and the singing genome. *Science* **346**:1256780.
1190 doi:10.1126/science.1256780
1191 Wilson EO. 1971. The insect societies. Cambridge: Harvard University Press.
1192 Wilson EO. 1980. Caste and division of labor in leaf-cutter ants (Hymenoptera: Formicidae:
1193 *Atta*). *Behav Ecol Sociobiol* **7**:157–165. doi:10.1007/BF00299521
1194 Woodard SH, Fischman BJ, Venkat A, Hudson ME, Varala K, Cameron SA, Clark AG,
1195 Robinson GE. 2011. Genes involved in convergent evolution of eusociality in bees. *Proc*
1196 *Natl Acad Sci* **108**:7472–7477. doi:10.1073/pnas.1103457108
1197 Zayed A, Robinson GE. 2012. Understanding the relationship between brain gene expression and
1198 social behavior: Lessons from the honey bee. *Annu Rev Genet* **46**:591–615.
1199 Zhu LJ, Christensen RG, Kazemian M, Hull CJ, Enuameh MS, Basciotta MD, Brasefield JA,
1200 Zhu C, Asriyan Y, Lapointe DS, Sinha S, Wolfe SA, Brodsky MH. 2011. FlyFactorSurvey:
1201 A database of *Drosophila* transcription factor binding specificities determined using the
1202 bacterial one-hybrid system. *Nucleic Acids Res*. doi:10.1093/nar/gkq858
1203
1204
1205
1206

1207 **Table 1.** Description of 15 candidate TFs regulating specialist behavioral phenotypes in Fig. 5.
1208 Names given are for *Drosophila melanogaster* motifs (Zhu et al. 2011), with homology to honey
1209 bee genes as in Kapheim et al. (2015). Function summaries are adapted from *D. melanogaster*
1210 gene annotations from FlyBase (release FB2020_05; FlyBase Consortium et al., 2019). Note that
1211 terms related to "regulation of transcription" apply to most TFs but were omitted for brevity.
1212

Motif	TF name	Function(s)
cwo	*clockwork orange*	circadian regulation of gene expression; dendrite morphogenesis
tai/met	*taiman, Mondo*	ecdysone receptor co-activator; lipid and carbohydrate metabolism
side	*sidestep, E(spl)mgamma-HLH*	pattern specification; neurogenesis; neuronal stem cell maintenance
h	*hairy*	cell morphogenesis; tracheal system development; cellular metabolism
sr	*stripe*	central nervous system development
max	*Max*	cell and organismal growth
dpn	*deadpan*	adult locomotory behavior; neuroblast development
usf	*Usf*	[unknown]
med	*Medea*	dorsal-ventral patterning; activin receptor signaling; eye morphogenesis; germ-line stem cell division and maintenance; neuron development
opa	*odd paired*	embryogenesis; midgut development; adult head morphogenesis; neural stem cell development; circadian rhythm
bab1	*bric a brac 1*	pattern formation; ovary morphogenesis; abdominal pigmentation; olfactory receptor neuron fate diversity
deaf1	*Deformed epidermal autoregulatory factor-1*	embryo development; regulation of immune response
crebA	*Cyclic-AMP response element binding protein A*	salivary gland development; cuticle development
sug	*sugarbabe*	regulates expression of insulin-like peptides and genes involved in lipid and carbohydrate metabolism
usp	*ultraspiracle*	cell migration; response to ecdysone; germ cell development; metamorphosis; mushroom body development; neuron remodeling

1213
1214
1215
1216
1217
1218
1219
1220

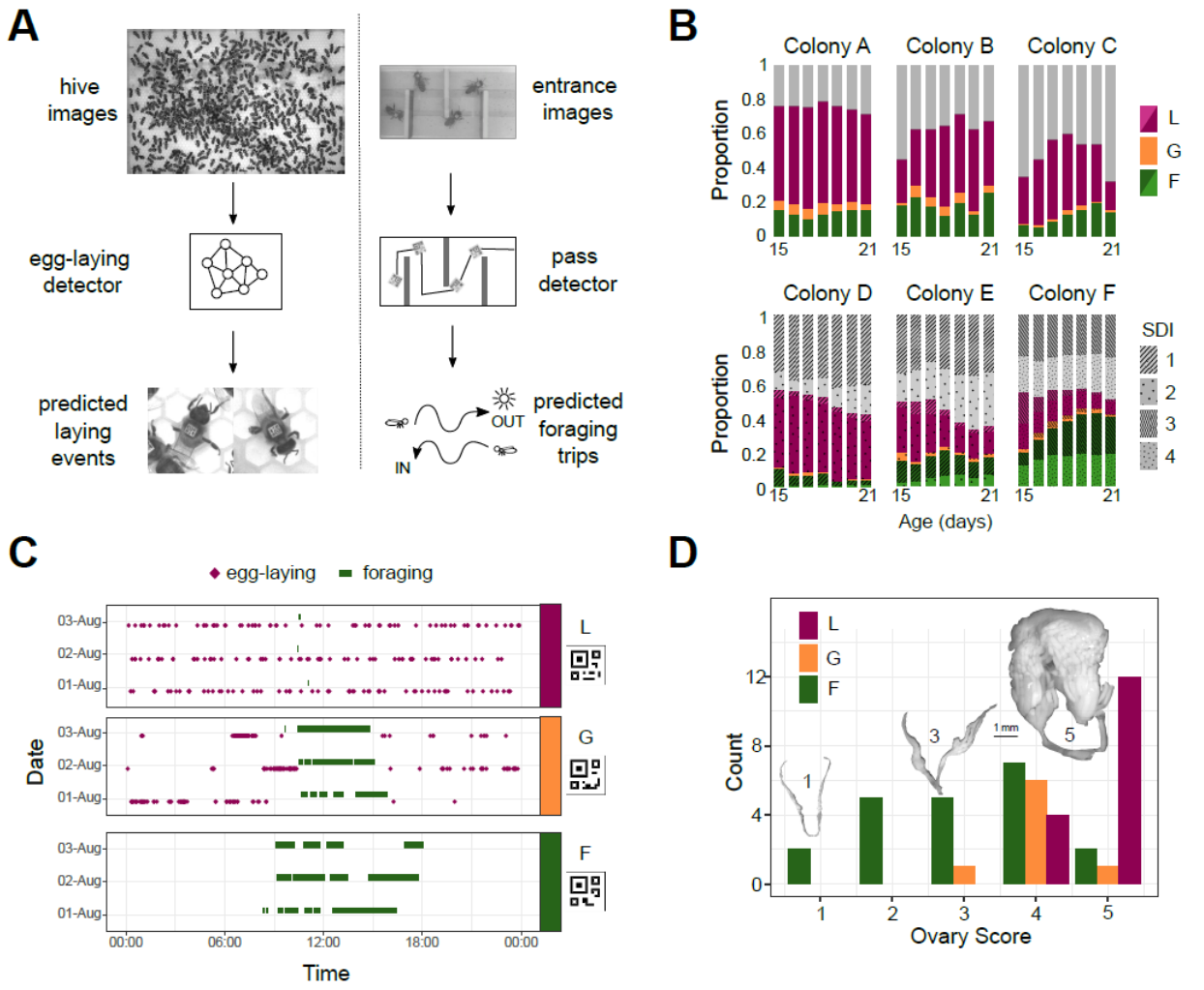

Figure 1. Automated monitoring of behavior in queenless colonies of laying worker honey bees. **(A)** Automatic behavior monitoring was performed inside the hive and at the hive entrance to predict egg-laying and foraging events in six colonies (N=800 bees per colony at the start of each trial). Hive images were captured 1/s for 24 h/day, and entrance images 2/s for 12 h/day beginning when adult bees were 15 days old. **(B)** Proportion of bees alive each day categorized as layers (purple), foragers (green), generalists (orange), or others (gray). For colonies A-C, individuals were from single source colonies headed by a naturally mated queen. For colonies D-F, individuals from two source colonies headed by queens each inseminated by semen from a single different drone (single drone inseminated, SDI) were mixed. Different source colonies are indicated by pattern and hue. **(C)** Ethograms for three individuals selected for sequencing (bCodes shown below group labels) across three days of tracking. **(D)** Distribution of ovary scores for individuals selected for sequencing. Insets are images from bees with ovary scores of 1, 3, and 5. L: layer, G: generalist, F: forager.

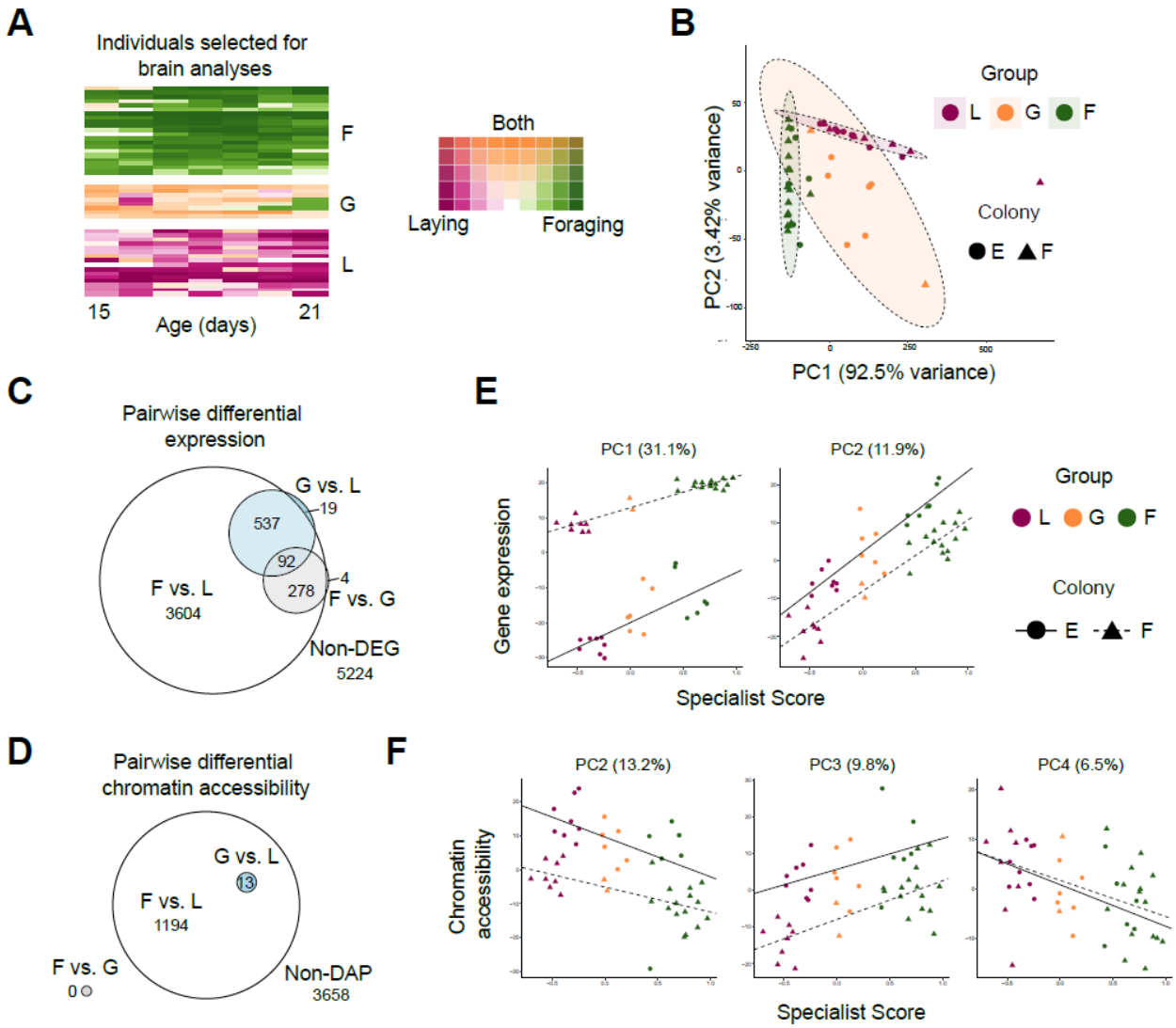

Figure 2. Patterns of brain gene expression and chromatin accessibility are associated with behavior. **(A)** Daily rank-normalized behavior of individuals (rows) selected for brain RNAseq and ATACseq analysis converted to 2D colorspace from specialist and generalist scores. **(B)** Principal Component Analysis (PCA) of behavioral variation for individuals chosen for brain RNAseq and ATACseq analysis. Metrics included number of eggs laid, number of foraging events, proportion of foraging trips with evidence of nectar collection, proportion of trips with evidence of pollen collection, and proportion of trips with evidence of both nectar and pollen collection. **(C)** Euler diagram for overlaps of pairwise differentially expressed genes (DEGs) between behavioral groups. Note that one gene was overlapping between F vs. G and G vs. L (but not F vs. L) and is not represented in the diagram due to graphical constraints. **(D)** Euler diagram for overlaps of genes proximal to pairwise differentially accessible chromatin peaks (DAPs) between behavioral groups. **(E)** PCs from PCA of brain transcriptomic profiles regressed against specialist score (PC1: R^2=0.947, p<0.0001; PC2: R^2=0.838, p<0.001). **(F)** PCs from PCA of brain chromatin accessibility regressed against specialist score (PC2: R^2=0.584, p<0.001; PC3: R^2=0.543, p<0.0001; PC4: R^2=0.187, p<0.0045; PC1: p>0.05). L: layer, G: generalist, F: forager.

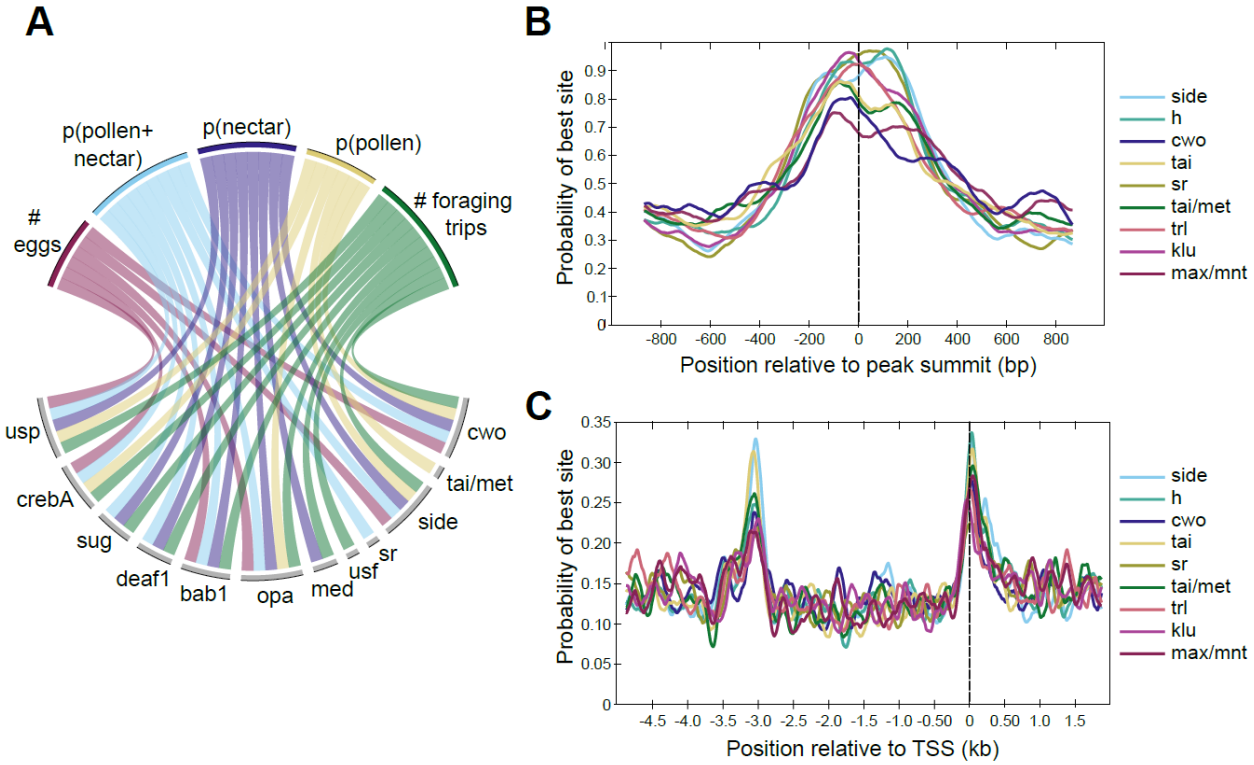

Figure 3. Differences in TF activity and TF motif occurrence are associated with specific behavioral phenotypes. **(A)** Circos plot representing a subset of significant correlations between behaviors (top) and expression of TF modules (bottom). Lines connecting behaviors with TF modules indicate significant associations. TF modules included are those mentioned in the main text or in other figures, and five of nine traits are included for simplicity. All significant correlations between behaviors and TF modules are given in Table S8. For behaviors, p indicates proportion (e.g., p(pollen) is the proportion of returning foraging trips where the bee carried pollen). **(B)** Motifs enriched within DAPs show maximum binding probabilities near peak summits. **(C)** Motifs enriched in promoter regions of forager>layer DEGs show elevated binding probabilities ~3kb upstream of and overlapping TSSs. Motif names and sequences are from FlyFactor (Zhu et al. 2011) for *Drosophila melanogaster*.

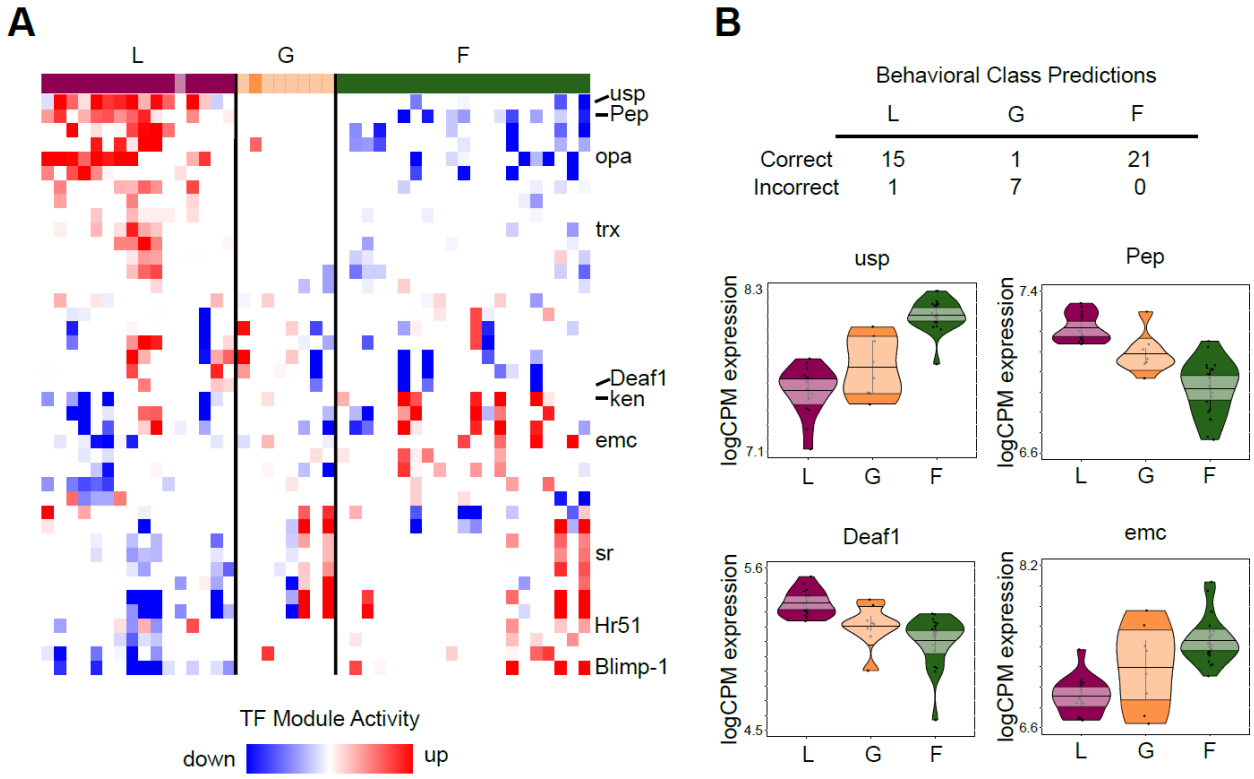

Figure 4. TF module activity and TF expression predict individual variation in behavior. **(A)** TF modules (rows) with significant up/downregulation in at least 10 individuals, sorted by hierarchical clustering. Individuals (columns) are ordered by specialist score, with darkly colored blocks indicating correctly classified individuals based on TF expression prediction analysis and lightly colored blocks indicating incorrect classification. TF modules showed patterns of differentiation between L and F, while G were more variable in module activity. Labeled modules are those with TFs shown in panel (B) or discussed in text. **(B)** Class prediction analysis based on brain TF expression correctly classified all but one specialist (L: layer, F: forager) but only one generalist (G). Normalized expression (logCPM) of 4 of the top 20 informative TFs for class prediction analysis are shown (others in Fig. 4 – figure supplement 1). Median of points is represented by bold horizontal line within shaded 95% confidence interval, with length of shape and smoothed curve showing range and density of data, respectively.

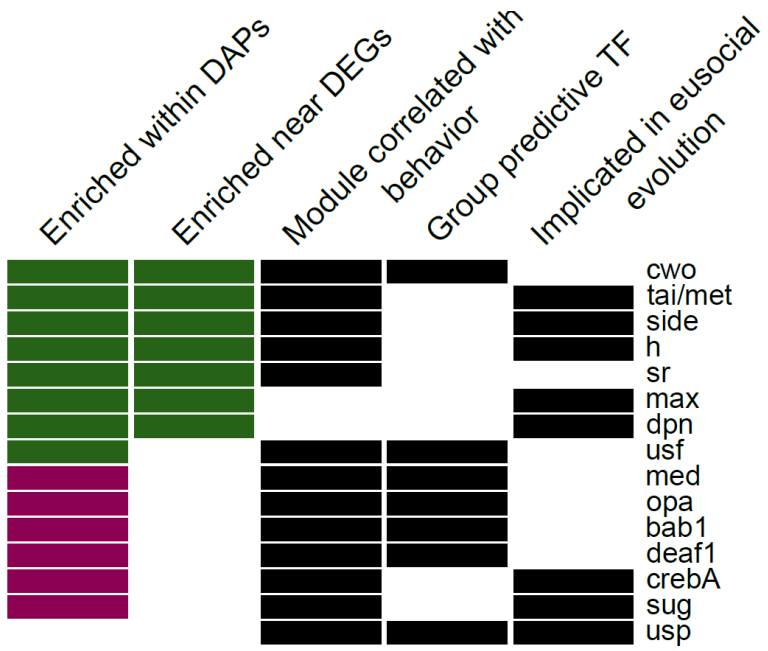

Figure 5. Fifteen candidate TFs predicted to regulate egg-laying and foraging behavior based on evidence across analyses (descriptions of categories in Materials and methods). Names given are for *Drosophila melanogaster* motifs (Zhu et al. 2011), with homology to honey bee genes as in Kapheim et al. (2015). Color of bar in first two columns indicates whether there was stronger enrichment among forager-biased (green) or layer-biased (purple) peaks or genes.

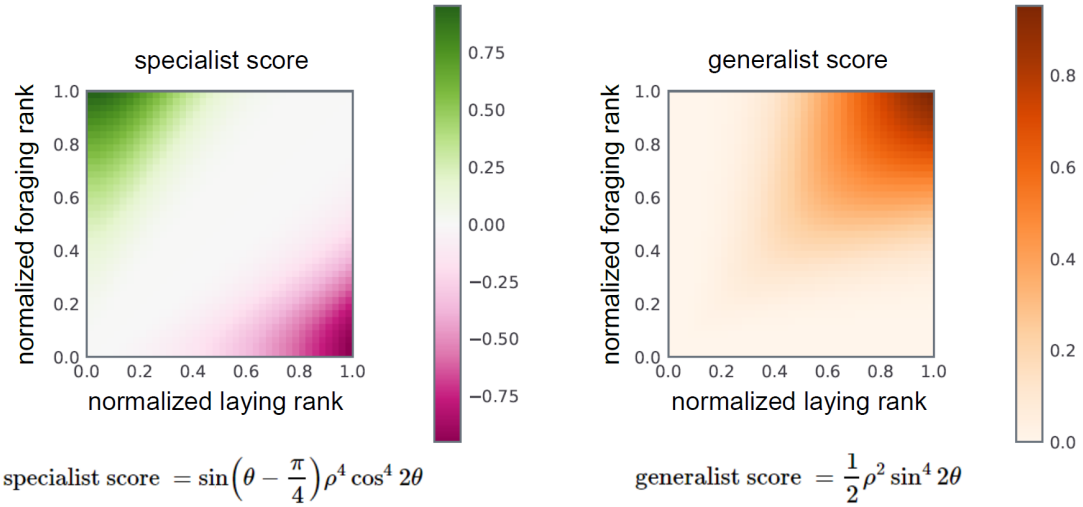

$$\text{specialist score} = \sin\left(\theta - \frac{\pi}{4}\right)\rho^4 \cos^4 2\theta$$

$$\text{generalist score} = \frac{1}{2}\rho^2 \sin^4 2\theta$$

Figure 2- figure supplement 1. Formulae and color-space mapping for specialist (left) and generalist (right) behavioral scores.

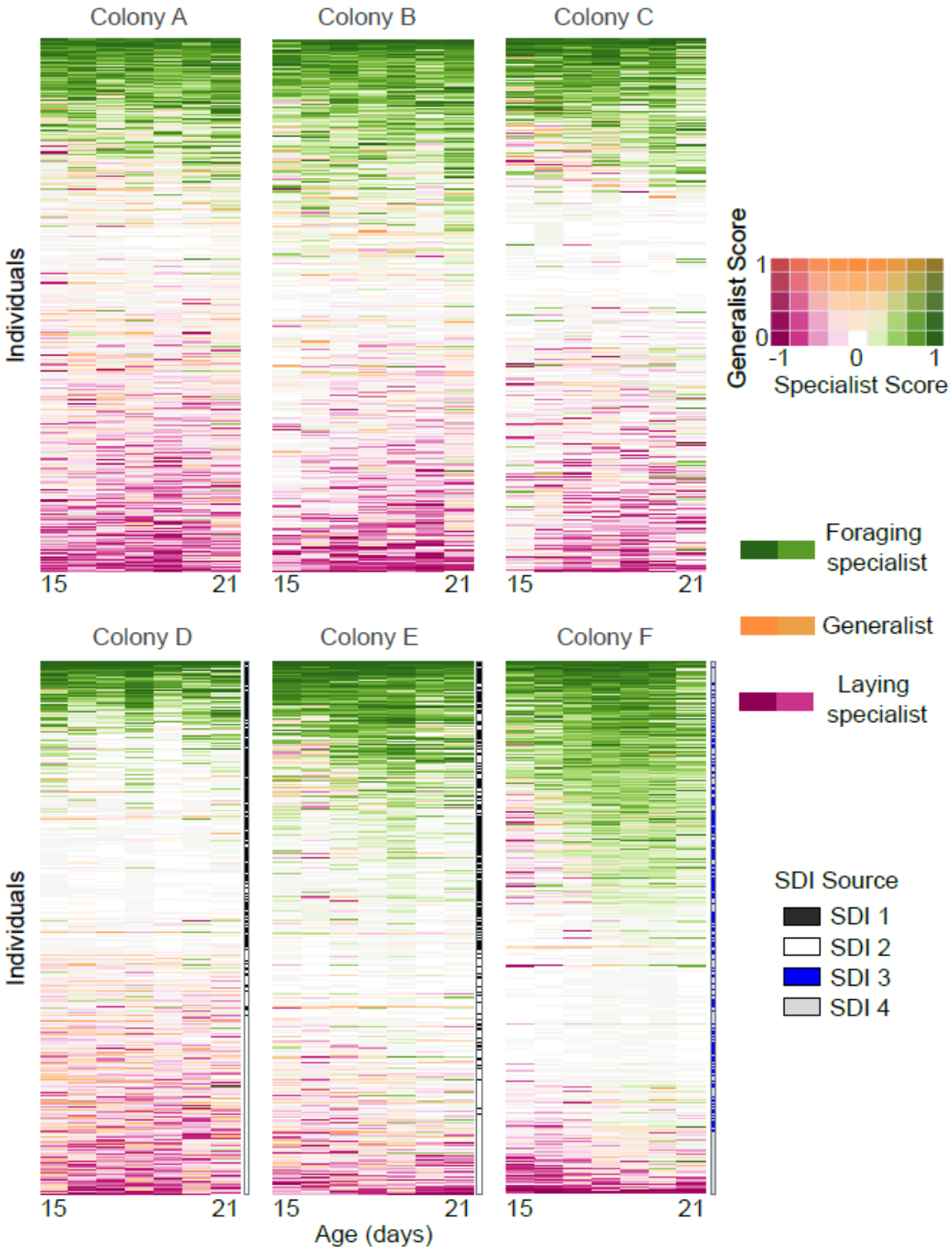

Figure 2- figure supplement 2. Daily behaviors of individual bees (rows) across time in each colony. Colored rectangles indicate specialist and generalist scores represented in 2D color space as shown in legend. Individuals are sorted by median lifetime specialist score. Single-drone inseminated (SDI) queen source is shown to the right of each row for colonies D-F, where workers were known offspring of two SDI queens per colony. In colonies A-C workers were offspring of naturally mated queens.

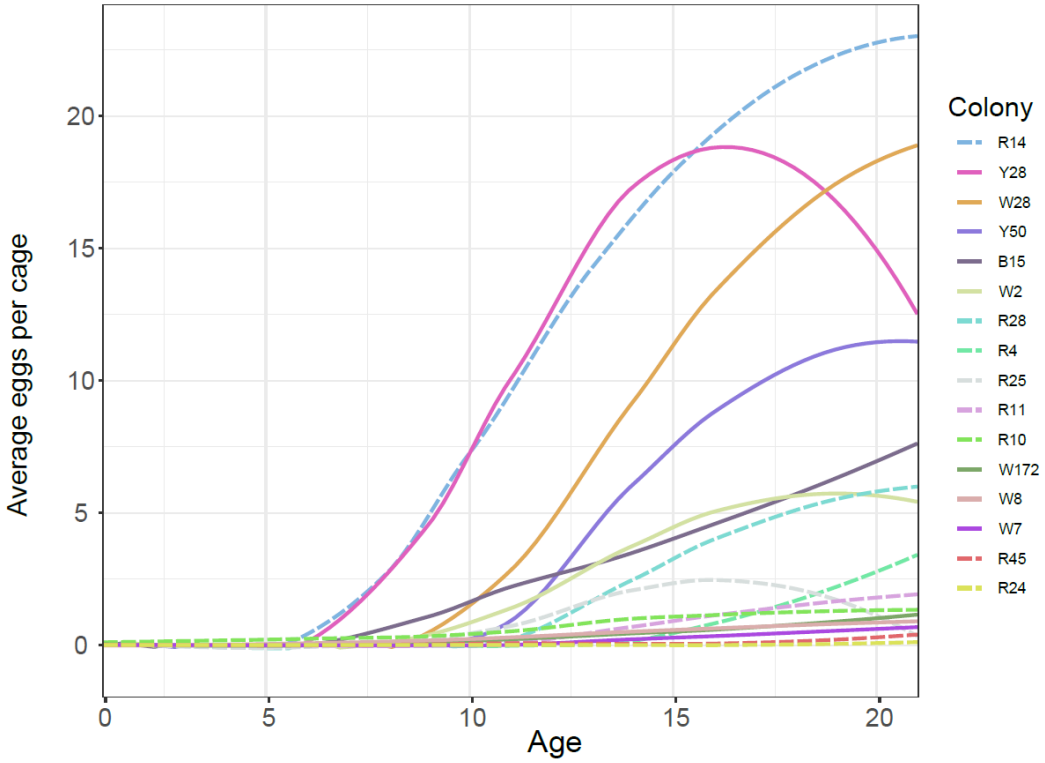

Figure 2- figure supplement 3. Smoothed average egg counts for laying workers in laboratory cages. Solid lines indicate bees from source colonies headed by a naturally-mated queen, while dashed lines indicate bees from source colonies headed by queens instrumentally inseminated with semen from a single drone (SDI). Colonies used as sources for behavioral tracking included W28, W2, R25, and R45.

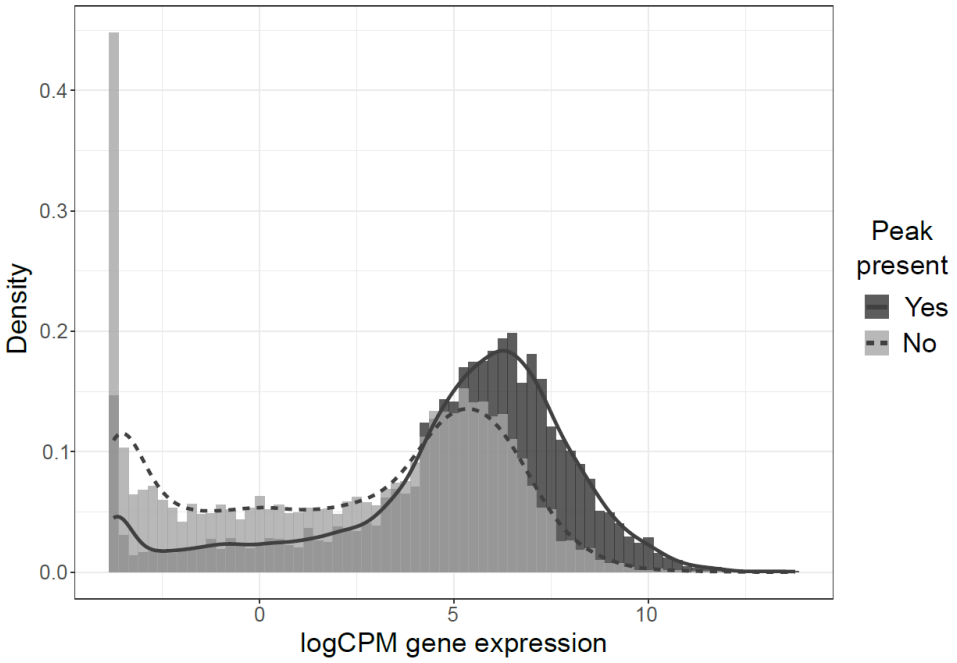

Figure 2- figure supplement 4. Histogram (bars) and density (lines) of normalized (logCPM) gene expression for genes with (dark gray) and without (light gray) nearby peaks of chromatin accessibility. Distributions are significantly different ($p<0.0001$, Kolmogorov-Smirnov test).

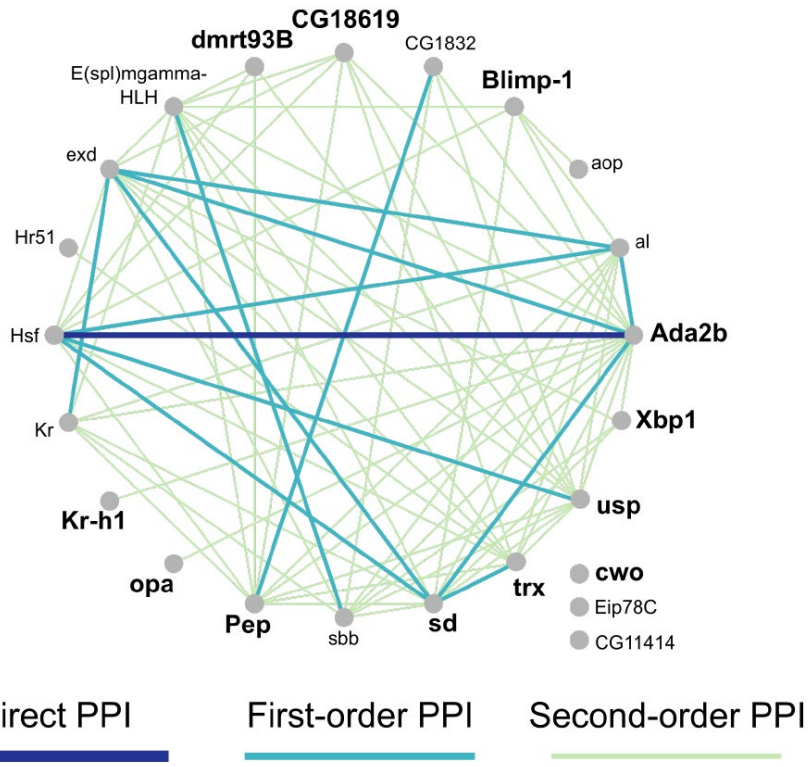

Figure 3- figure supplement 1. Network of 23 TFs with module expression significantly correlated with 9 behavioral and physiological metrics (see Supplementary File 2) measured across individuals. Edges indicate known interactions based on MIST database for *Drosophila melanogaster*. First-order PPI indicates one intermediate protein between linked nodes, while second-order PPI indicates two intermediate proteins. PPI = protein-protein interaction.

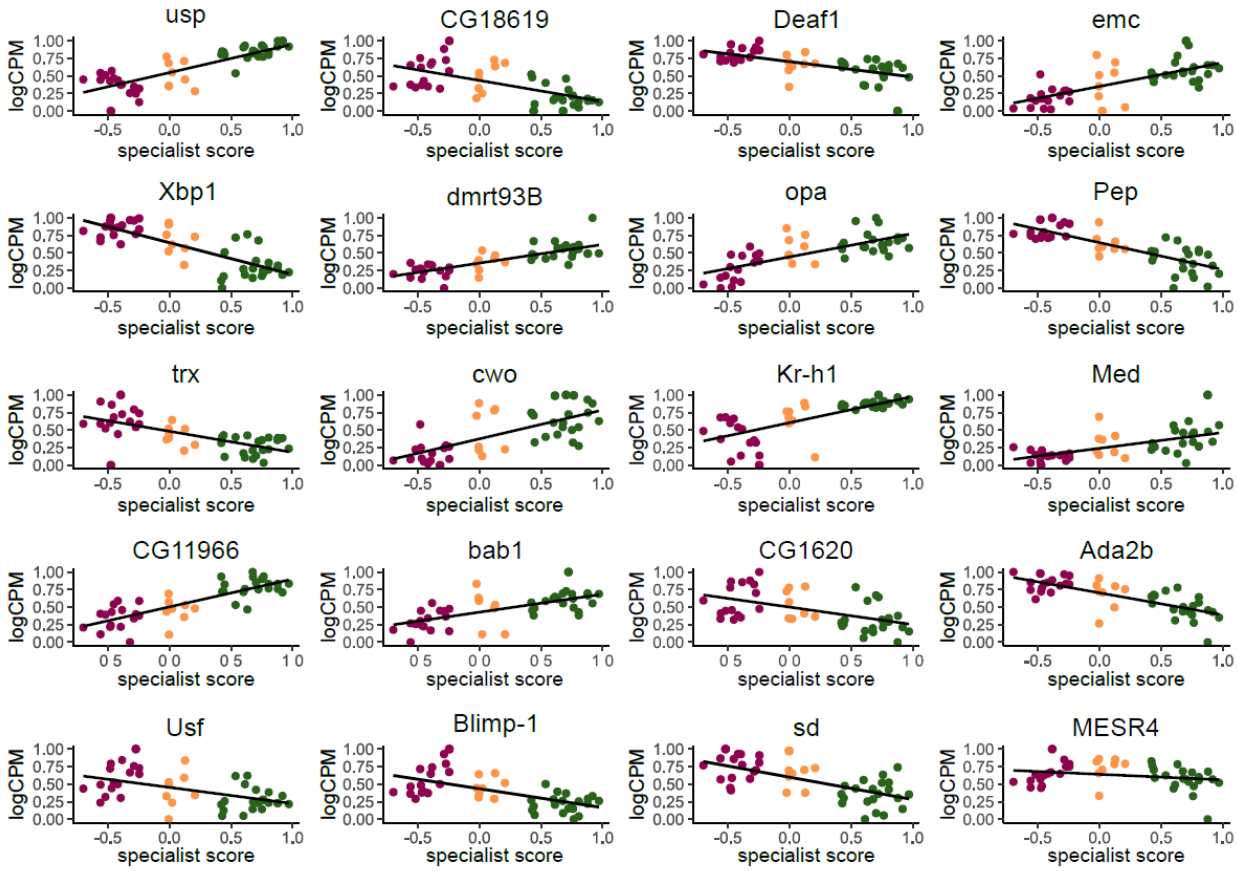

Figure 4- figure supplement 1. Normalized expression (logCPM, scaled to a maximum of 1 to allow for comparison across TFs) of the top 20 most informative TFs for class prediction analysis plotted against individual specialist score. Points are colored by behavioral group (Layer: purple, Generalist: orange, Forager: green). Although some of the top predictors individually show weak correlation with specialist score, the random forest machine learning algorithm combined multiple weak predictors together in a single model to accurately classify the three behavioral groups, suggesting the TFs act combinatorially to influence behavior.

1409 **Supplemental Files**

1410 **Supplementary File 1:** Daily egg-laying counts, foraging counts, specialist scores, and
1411 generalist scores for individual bees

1412 **Supplementary File 2:** Detailed behavioral and physiological information for sequenced bees

1413 **Supplementary File 3:** Differentially expressed genes (DEGs) and Gene Ontology (GO)
1414 enrichment of DEGs for each pairwise comparison of specialists and generalists

1415 **Supplementary File 4:** Differentially accessible peaks (DAPs) and Gene Ontology (GO)
1416 enrichment of DAPs for each pairwise comparison of specialists and generalists

1417 **Supplementary File 5:** Lists of genes with upper and lower 5% of PC loadings for gene
1418 expression and Gene Ontology (GO) enrichment results

1419 **Supplementary File 6:** Lists of genes with upper and lower 5% of PC loadings for chromatin
1420 accessibility and Gene Ontology (GO) enrichment results

1421 **Supplementary File 7:** TF motif enrichment of DAPs and DEGs

1422 **Supplementary File 8:** Predicted gene regulatory network (GRN), GRN module correlations
1423 with behavior and physiological measurements, and importance scores of TFs from class
1424 prediction analysis

1425 **Supplementary File 9:** Overlaps and statistics for comparative gene expression datasets

1426 **Supplementary File 10:** Details of experimental setup for recorded colonies